

CHAPTER III

RESULTS AND DISCUSSION

We have studied the effect of aging time and effect of annealing on the rheological and optical properties of several emulsion systems as a function of aging time and temperature. The systems studied are as follow.

1) Effect of Aging Time

System	CTAC (%wt/wt)	BTAC (%wt/wt)	FA (%wt/wt)	HEC (%wt/wt)
CTAC/FA	1.0	-	2.0-8.0%	-
BTAC/FA	-	1.0	2.0-8.0%	-
CTAC/FA/HEC	1.0	-	2.0-8.0%	0.5

2) Effect of Annealing

System	CTAC (%wt/wt)	BTAC (%wt/wt)	FA (%wt/wt)	HEC (%wt/wt)
CTAC/FA	1.0	-	2.0-5.0%	-
BTAC/FA	-	1.0	2.0-5.0%	-
CTAC/FA/HEC	1.0	-	2.0-5.0%	0.5

3.1 Effect of Aging Time

3.1.1 Emulsions at low fatty alcohol concentration

Figure 3.1 shows the zero shear rate viscosity as a function of aging time of different emulsion systems. For the CTAC/FA system, the zero shear rate viscosity slightly increases with aging time until reaching equilibrium. For BTAC/FA system, the zero shear rate viscosity slightly increases in period of 7 days and increases its value by a factor of two at 14 days before reaching equilibrium. In the case of CTAC/FA/HEC system, the zero shear rate viscosity slightly increases during a period of 7 days and sharply rises to a high shear rate viscosity value at 14 days. This system reaches the equilibrium after about 21 days.

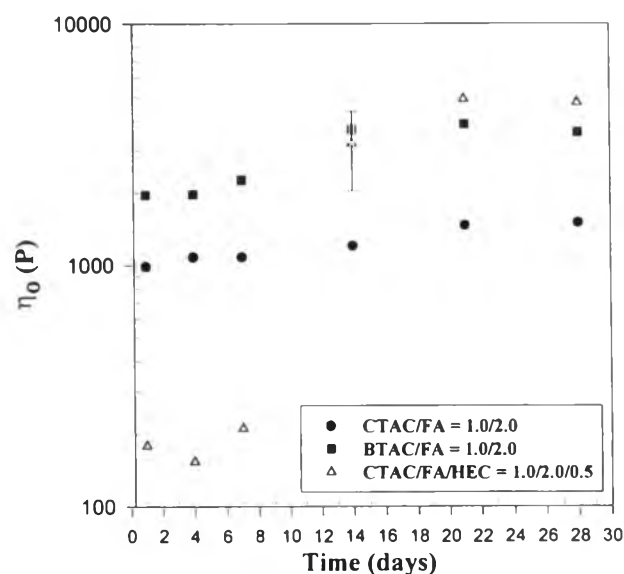


Figure 3.1 Zero shear rate viscosity vs. aging time for low FA emulsion systems.

3.1.2 Emulsions at high fatty alcohol concentration

Figure 3.2 shows zero shear rate viscosities of CTAC/FA, BTAC/FA, and CTAC/FA/HEC emulsion systems as a function of aging time. It can be seen that zero shear rate viscosities of the three emulsion systems steadily increase during the period of 7 days and reach equilibrium values after about 14 days.

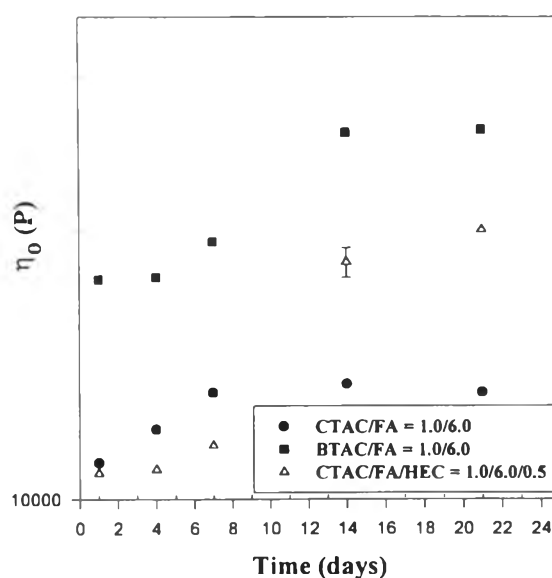










Figure 3.2 Zero shear rate viscosity vs. aging time for high FA emulsion systems.

Table 1. List of Symbols

	Micellar structure of CTAC
	Micellar structure of BTAC
	FA Monomer
	Excess FA
	Lamellar structure
	Vesicle structure
	Excess FA surrounded with lamellar aggregates
	HEC polymer chain

The micrographs of CTAC/FA system with low fatty alcohol are shown in Figure 3.3. Figure 3.3a shows micrographs of the lamellar aggregate structure that is formed by interaction between CTAC and FA. It can be seen that the structure size increases with aging time until it reaches equilibrium. The structures at low fatty alcohol concentration can be compared with proposed model in Figure 3.4. In this experiment, we used 1.0% of CTAC and the structure was presented in a micelle form. CTAC and FA interact with each other to form lamellar structure (Nakarapanich 1998). The lamellar structure size increases with aging time until reaching its equilibrium condition.

The micrographs of CTAC/FA system at high fatty alcohol concentration are shown in Figure 3.5. The structure size increases with aging time. Fatty alcohol can be seen to be in the middle of structures. We observed a network formation of lamellar structures after 14 days. Figure 3.6 shows the corresponding model from micrographs of CTAC/FA = 1.0/6.0 system. At high FA concentration, CTAC and FA interact with each other to form lamellar structure. Later on, the surfactant molecules penetrate into the middle to form a lamellar structure. Therefore, the size of excess fatty alcohol becomes smaller compared to the initial size. However, there is still some excess of FA at equilibrium. *Barry (1973) found that initially CTAC and FA can form the lamellar liquid crystalline phase by penetration of CTAC into molten FA. Later the unreacted CTAC will penetrate slowly into the crystalline alcohol to form additional network structure.*

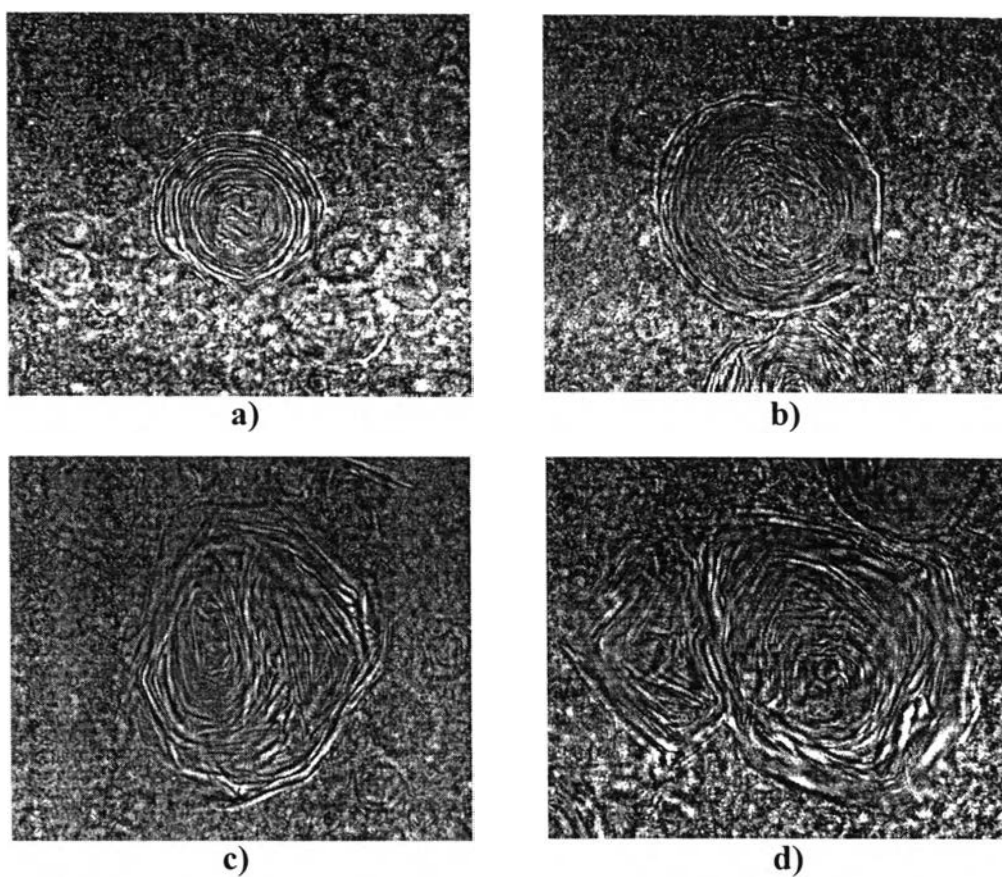


Figure 3.3 Micrographs of the CTAC/FA = 1.0/2.0 system structure as a function of aging time: a) 1 day; b) 7 days; c) 14 days; d) 21 days.

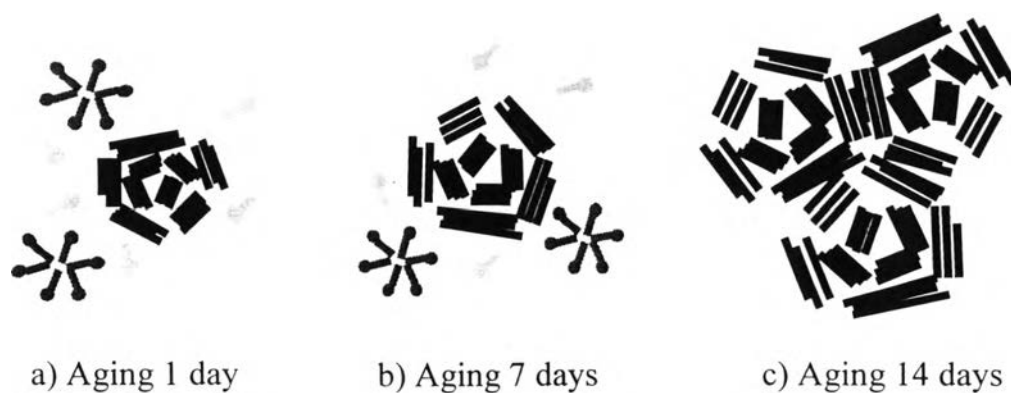


Figure 3.4 Proposed models of the CTAC/FA = 1.0/2.0 system as a function of aging time.

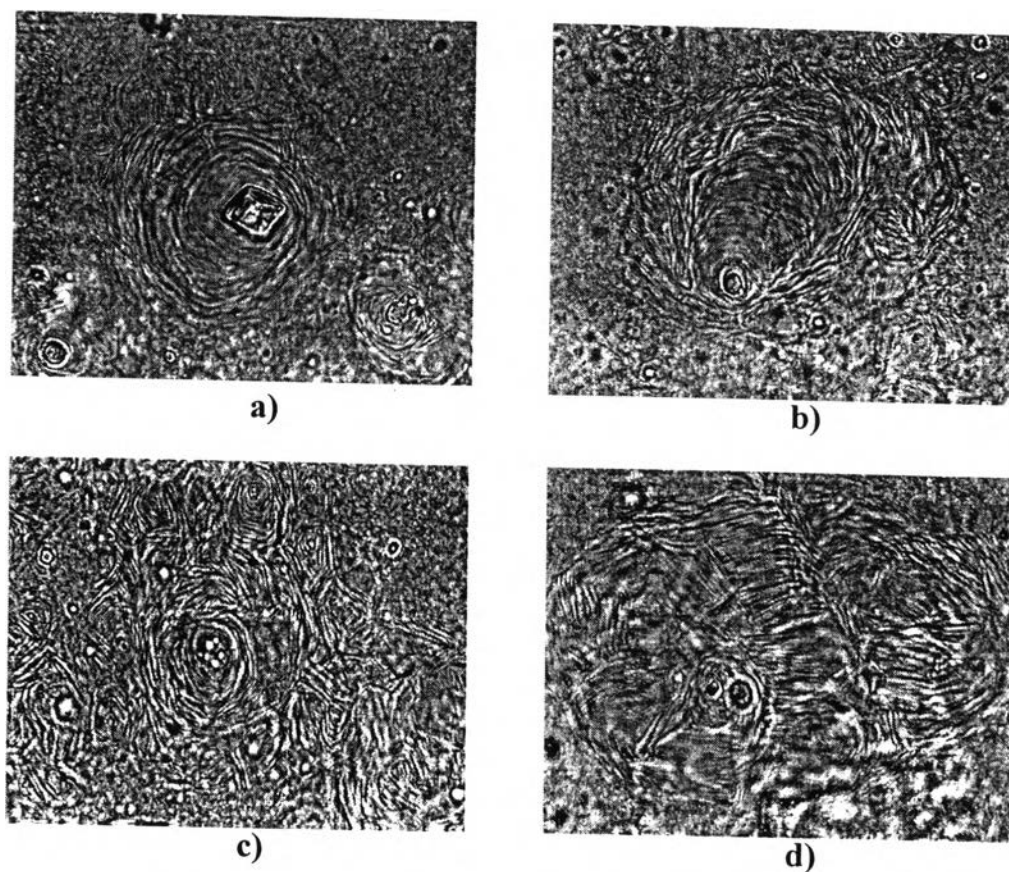


Figure 3.5 Micrographs of the CTAC/FA = 1.0/6.0 system structure as a function of aging time: a) 1 day; b) 7 days; c) 14 days; d) 21 days.

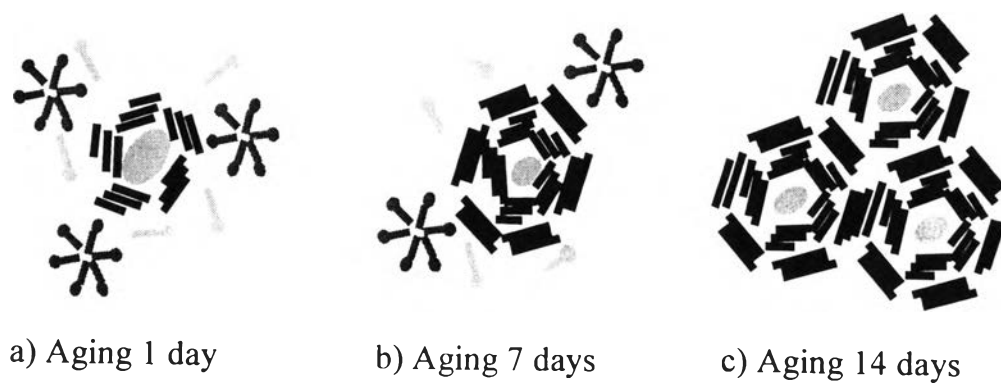


Figure 3.6 Proposed models of the CTAC/FA = 1.0/6.0 system as a function of aging time.

The micrographs of BTAC/FA system with low fatty alcohol concentration are shown in Figure 3.7. BTAC and FA interact with each other to form vesicle type of structure and its size increases with aging time. There is a small amount of excess fatty alcohol dispersed in the system when compared with the CTAC/FA system at the same FA concentration. Because BTAC has 22 carbon atoms and is not compatible with FA containing 16 carbon atoms; therefore, the interaction between CTAC and FA is more pronounced. Figure 3.8 shows the corresponding model from micrographs of the BTAC/FA = 1.0/2.0 system. At low fatty alcohol concentration, the structures differ from the CTAC/FA system. These structures are similar to the continuous lamellar phase formation. The structure size increase with aging time.

The micrographs of BTAC/FA system with high fatty alcohol concentration are shown in Figure 3.9. We can observe that the lamellar aggregate forms surrounding the crystalline FA. The structures of this system differ from that of the CTAC/FA system due to the difference in the type of cationic surfactant. At high FA concentration, there is more crystalline FA left in the middle of structure than the CTAC/FA system at the same fatty alcohol concentration because of the less favorable interaction between BTAC and FA. Figure 3.10 shows the corresponding models from micrographs of the BTAC/FA = 1.0/6.0 system. At the high fatty alcohol concentration, BTAC and FA interact with each other to form lamellar structures and consequently they have excess fatty alcohol left in the middle of the structure because of less preferable of interaction between BTAC and FA.

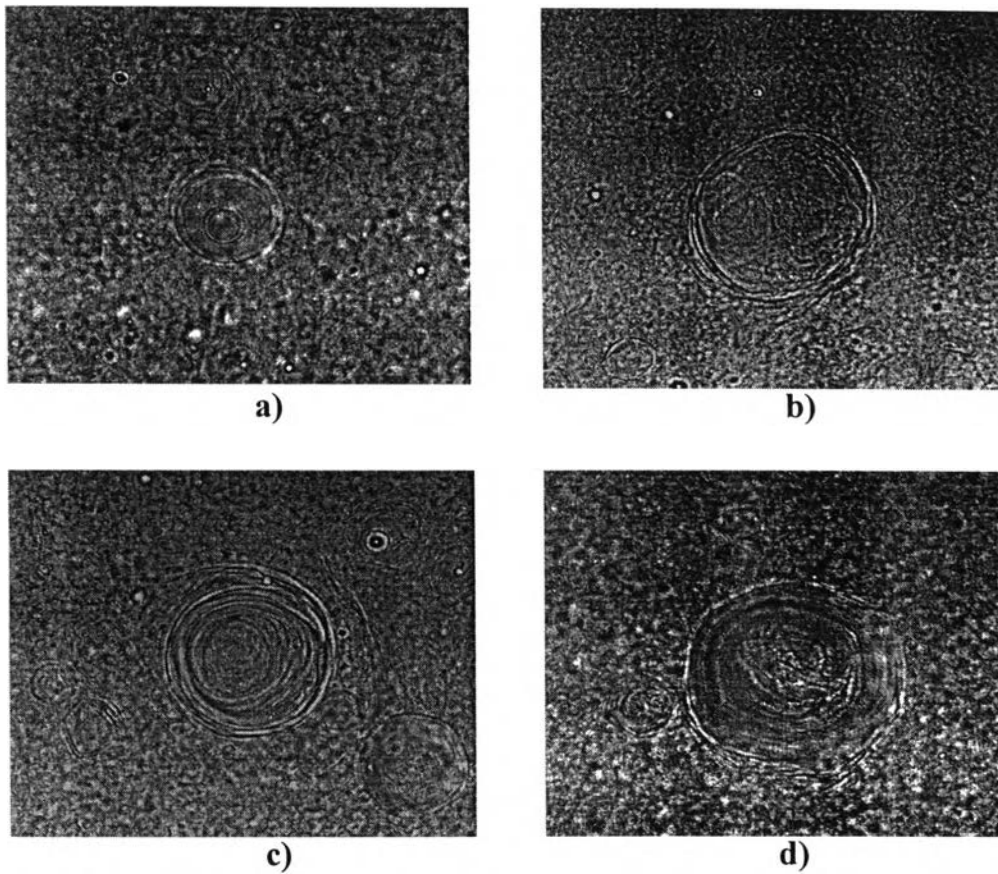


Figure 3.7 Micrographs of the BTAC/FA = 1.0/2.0 system structure as a function of aging time: a) 1 day; b) 7 days; c) 4 days; d) 21 days.

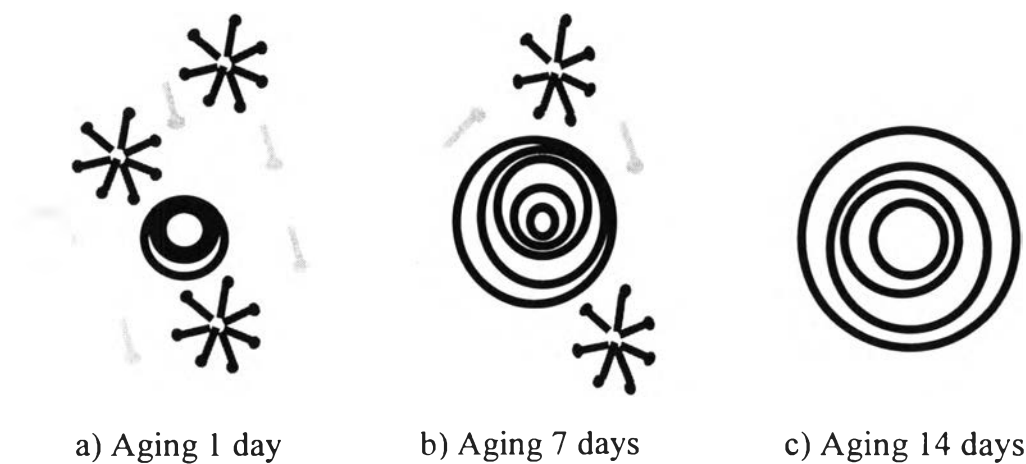


Figure 3.8 Proposed models of the BTAC/FA = 1.0/2.0 system as a function of aging time.

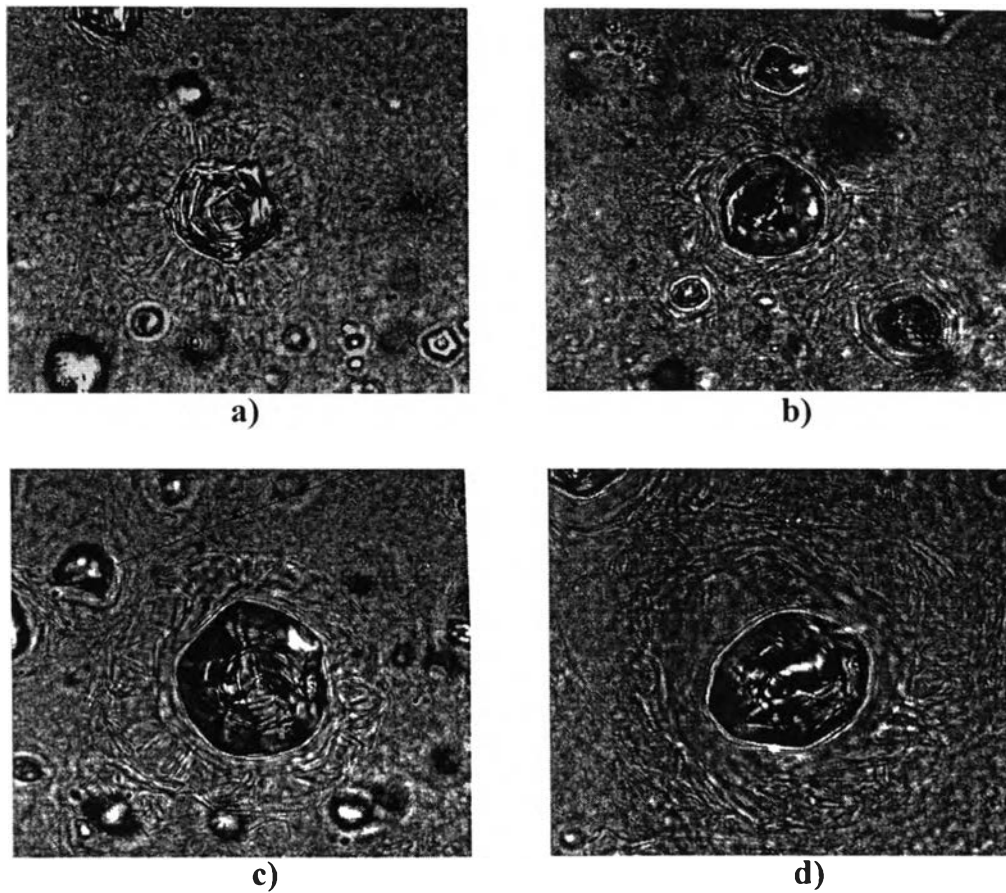


Figure 3.9 Micrographs of the BTAC/FA = 1.0/6.0 system structure as a function of aging time: a) 1 day; b) 7 days; c) 14 days; d) 21 days.

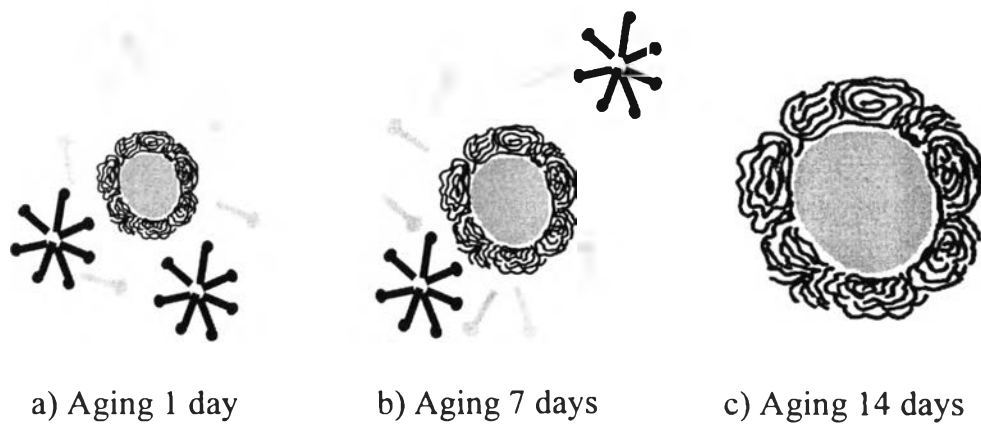


Figure 3.10 Proposed models of the BTAC/FA = 1.0/6.0 system as a function of aging time.

The micrographs of CTAC/FA/HEC system with low fatty alcohol concentration are shown in Figure 3.11. For low fatty alcohol concentration, we can observe the lamellar aggregate similar to that of the CTAC/FA system. But the structure size of the system with polymer is smaller than the system without polymer. This probably suggests that the polymer chain of HEC can interrupt the formation of lamellar structure. Figure 3.12 shows the corresponding model from micrographs of CTAC/FA/HEC 1.0/2.0/0.5 system. CTAC and FA interact with each other to form lamellar structure in the presence of HEC. The interaction between CTAC and FA takes longer time when compared to other systems because the HEC polymer chains disrupt and delay the formation of lamellar structure.

The micrographs of CTAC/FA/HEC with high fatty alcohol concentration are shown in figure 3.13. For high fatty alcohol concentration, there are partitions of lamellar aggregates. It can be suggested that the fatty alcohol induces the formation of lamellar structure. Furthermore, there is no aggregation of lamellar aggregate due to the polymer chain obstructing the structure aggregation. Figure 3.14 shows the corresponding model from micrographs of CTAC/FA/HEC =1.0/6.0/0.5 system. CTAC and FA interact with each other to form lamellar structure. In this system, the polymer will play two important roles: not only obstructing or delaying the lamellar formation but also disrupting the aggregation of lamellar structure.

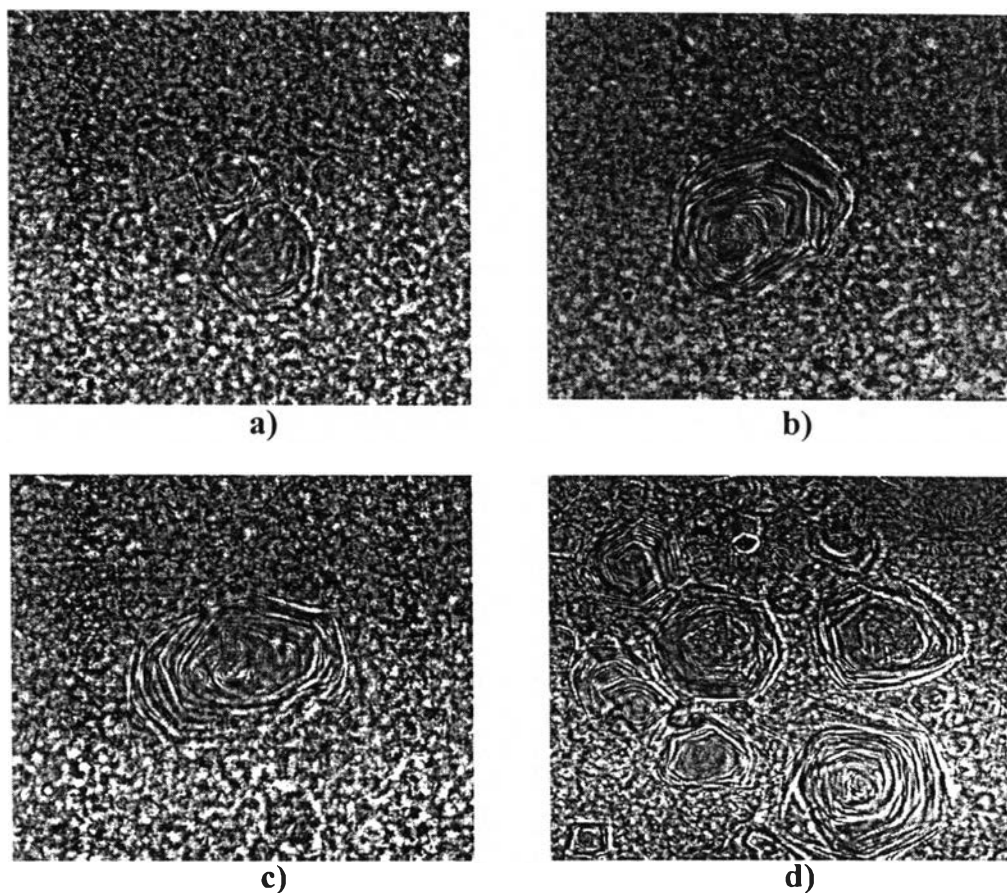


Figure 3.11 Micrographs of the CTAC/FA/HEC = 1.0/2.0/0.5 system structure as a function of aging time: a) 1 day; b) 7 days; c) 14 days; d) 21 days.

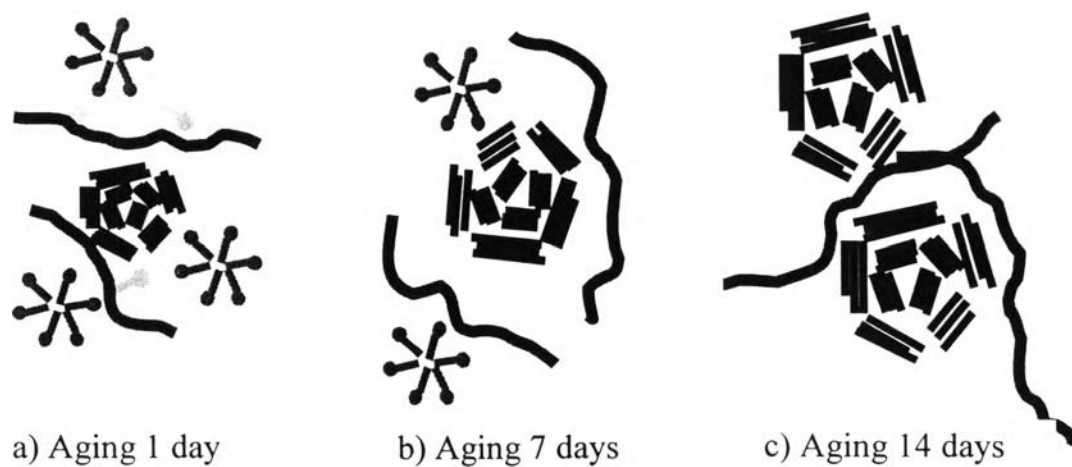


Figure 3.12 Proposed models of the CTAC/FA/HEC = 1.0/2.0/0.5 system as a function of aging time.

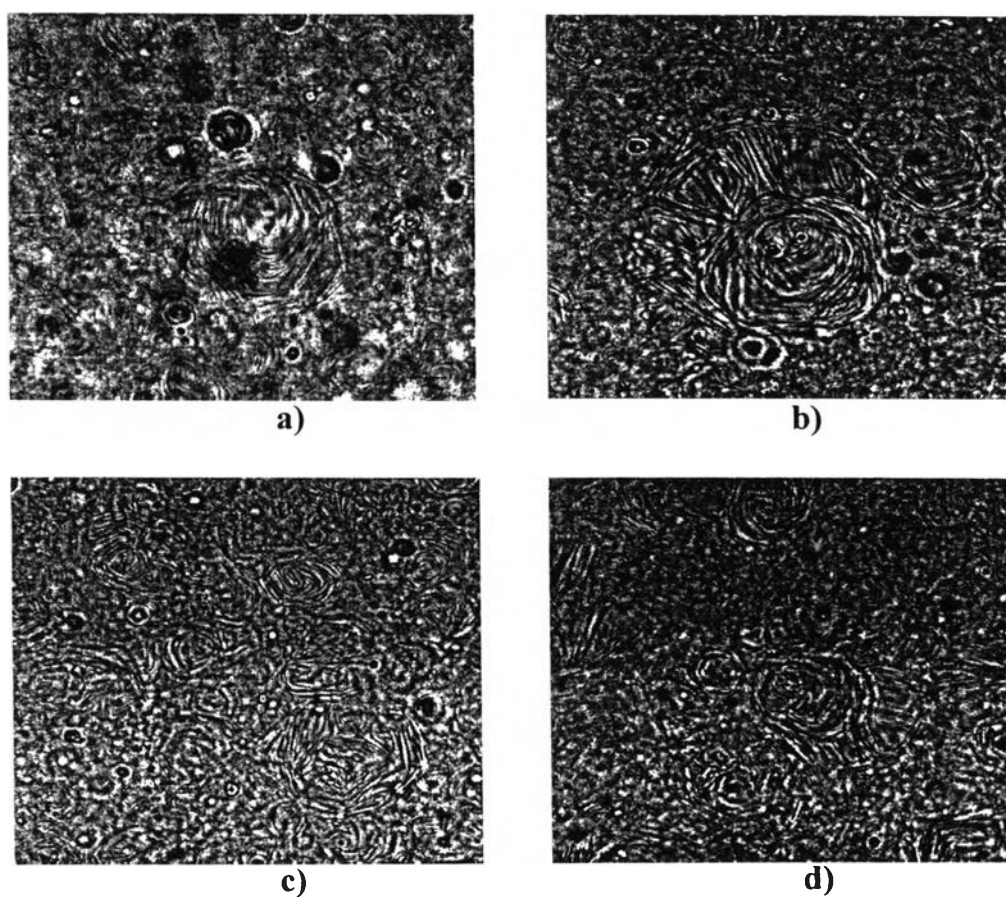


Figure 3.13 Micrographs of CTAC/FA/HEC = 1.0/6.0/0.5 system structure as a function of aging time: a) 1 day; b) 7 days; c) 14 days; d) 21 days.

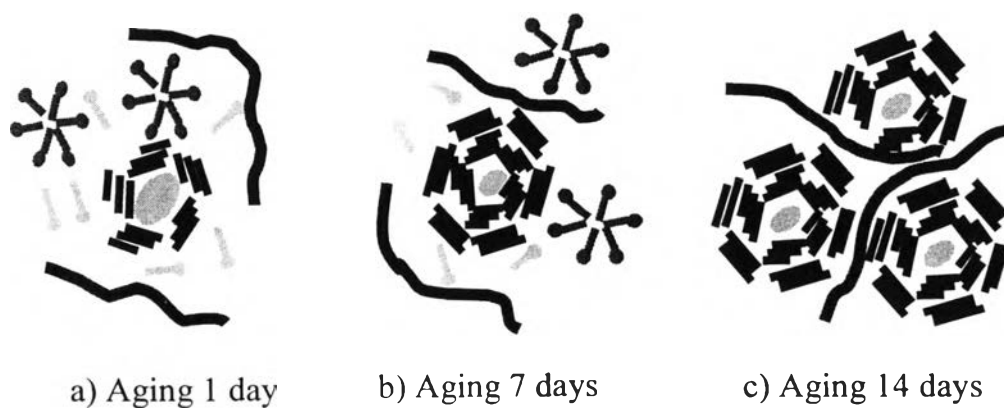


Figure 3.14 Proposed models of the CTAC/FA/HEC = 1.0/6.0/0.5 system as a function of aging time.

3.2) Effect of FA Concentration

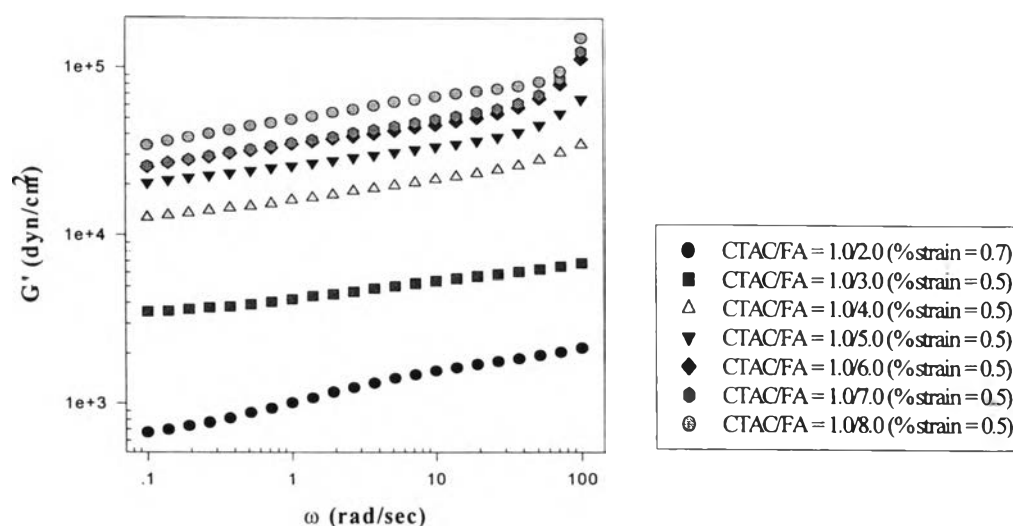


Figure 3.15 $G'(\omega)$ vs. frequency as a function of fatty alcohol concentration for CTAC/FA system at equilibrium.

Figure 3.15 shows $G'(\omega)$ versus frequency of CTAC/FA system as a function of FA concentration. It can be seen that the storage modulus increases at every frequency with increasing fatty alcohol concentration. This means that the emulsion elasticity increases with fatty alcohol content. We also found the upturn of $G'(\omega)$ at high frequency for CTAC/FA = 1.0/5.0-8.0% because the structure of CTAC/FA systems at high fatty alcohol concentration looks like a network type formation. Figure 3.16 shows that the $G''(\omega)$ increases with FA concentration. This indicates that the mixture becomes more viscous as well as more elastic.

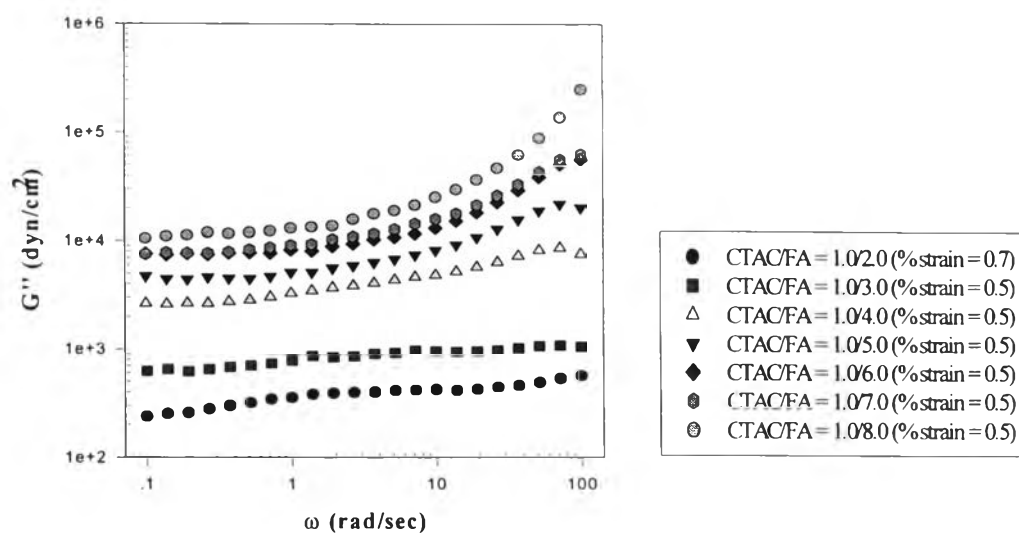


Figure 3.16 $G''(\omega)$ vs. frequency as a function of fatty alcohol concentration for CTAC/FA system at equilibrium.

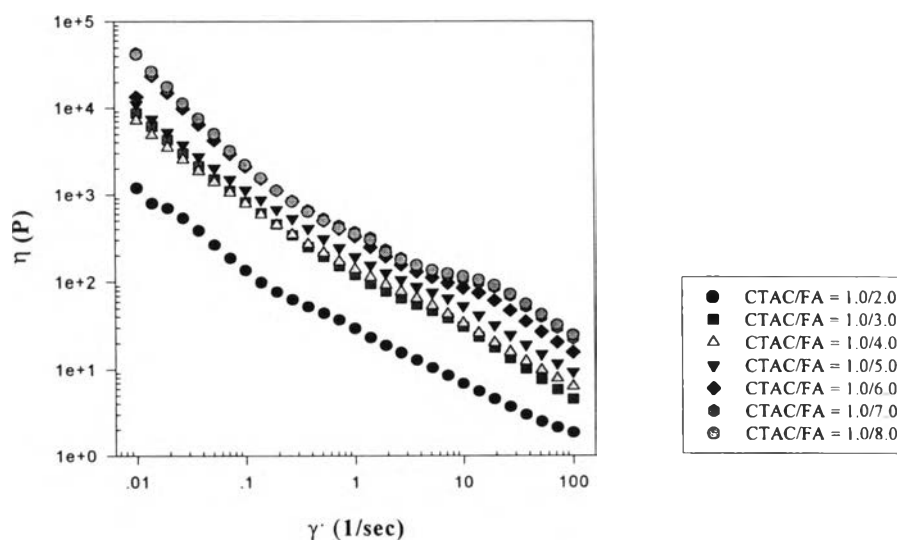


Figure 3.17 η vs. shear rate as a function of fatty alcohol concentration for CTAC/FA system at equilibrium.

Figure 3.17 shows the viscosity of CTAC/FA emulsion system versus shear rate as a function of fatty alcohol concentration. The viscosity profiles show shear-thinning behavior. They show a slight shoulder at shear rates between 1-20 s^{-1} . It is hypothesized that these shoulders appear due to residue fatty alcohol particles and the network type formation as shown in Figure 3.5c-d.

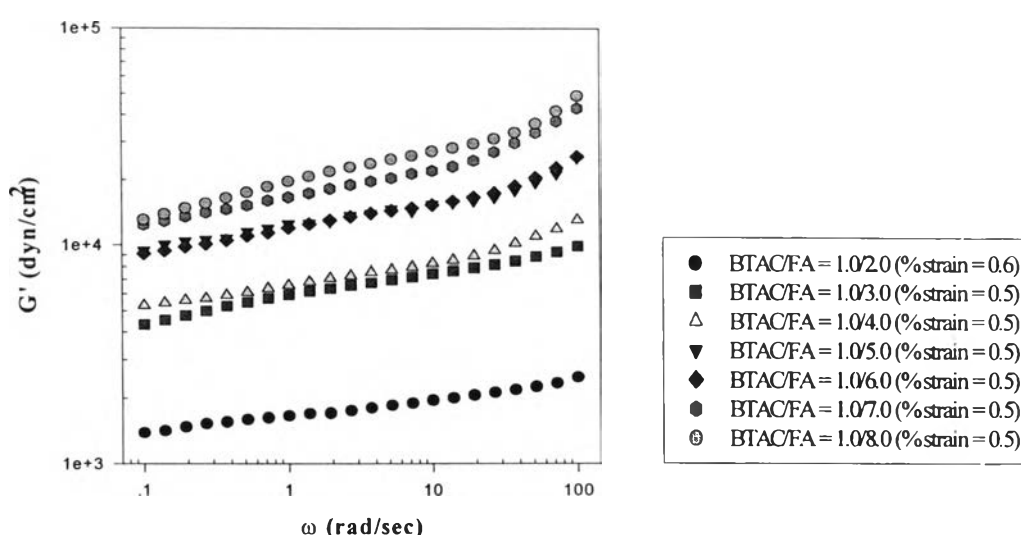


Figure 3.18 $G'(\omega)$ vs. frequency as a function of fatty alcohol concentration for BTAC/FA system at equilibrium.

Figure 3.18 shows $G'(\omega)$ versus frequency as a function of fatty alcohol concentration for BTAC/FA systems. The storage modulus increases with fatty alcohol concentration at all frequencies. We can observe that the upturn of $G'(\omega)$ at high frequencies for high fatty alcohol concentration. This implies that the bending of $G'(\omega)$ is a result of excess fatty and some structure formation as shown in Figure 3.9 c-d. $G''(\omega)$ also increase with fatty alcohol concentration as shown in Figure 3.19. They show the same trend as $G'(\omega)$. We can observe the bending of graphs at high frequency for the BTAC/FA systems as same as $G'(\omega)$.

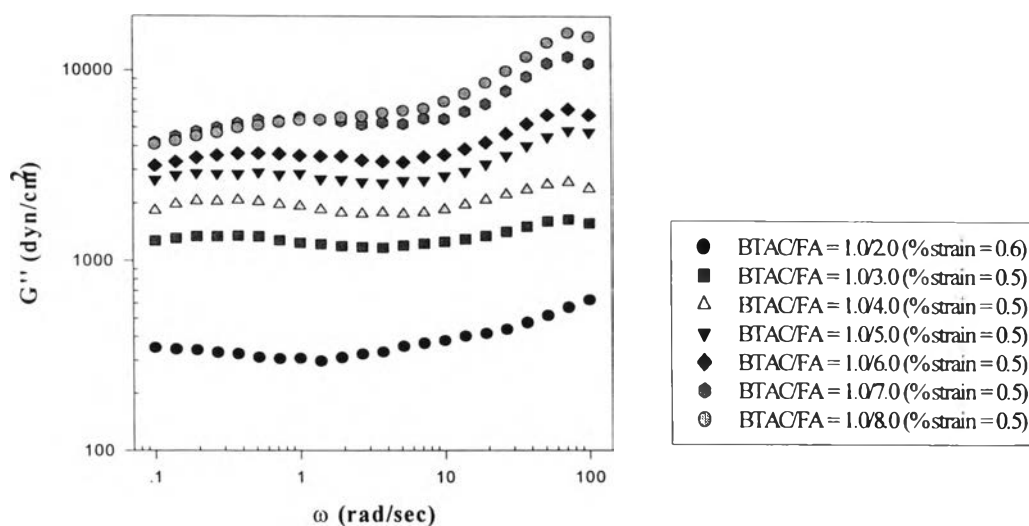


Figure 3.19 $G''(\omega)$ vs. frequency as a function of fatty alcohol concentration for BTAC/FA system at equilibrium.

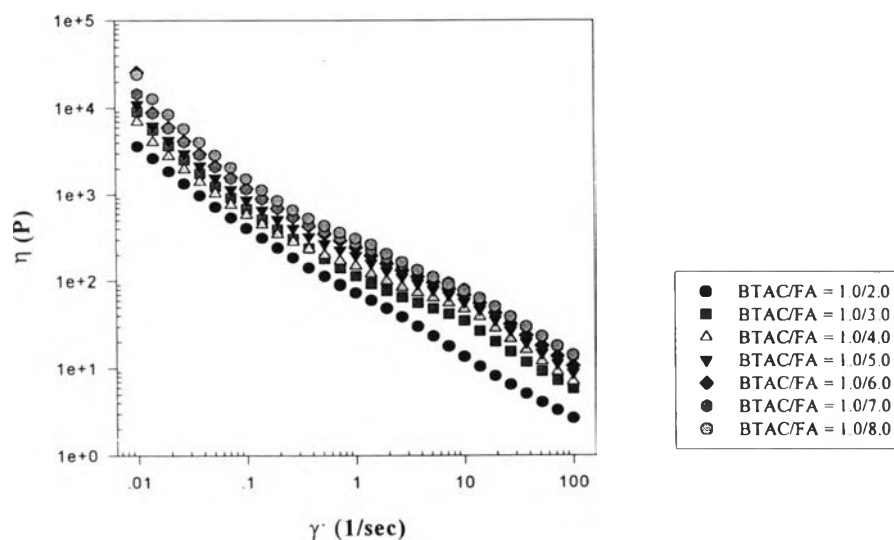


Figure 3.20 η vs. shear rate as a function of fatty alcohol concentration for BTAC/FA system at equilibrium.

Figure 3.20 shows the viscosity of emulsion BTAC/FA system as a function of fatty alcohol concentration. The viscosity profiles all show shear-thinning behavior. Viscosity at any shear rate increases with fatty alcohol concentration. We can observe a slight shoulder at shear rates between 1-10 sec^{-1} . This occurs due to the same reason as that of the CTAC/FA system.

3.3) Effect of Surfactant Chain Length

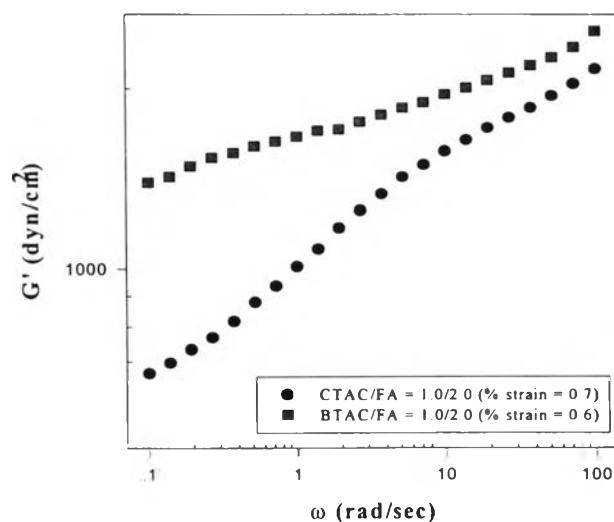


Figure 3.21 Comparison of $G'(\omega)$ between CTAC/FA and BTAC/FA systems at low fatty alcohol concentration at equilibrium.

Figure 3.21 shows comparison of $G'(\omega)$ between the CTAC/FA and BTAC/FA systems at surfactant concentration 1.0% and fatty alcohol concentration 2.0%. $G'(\omega)$ of the BTAC/FA system is higher than the CTAC/FA system at all frequency. This means that the emulsion elasticity of BTAC/FA is higher than CTAC/FA system at low FA concentration. This is probably because of the poorer solubility of FA in BTAC due to its longer surfactant chain length

which causes a decrease in lamellar network morphology (compare Fig.3.7d versus Fig. 3.3d).

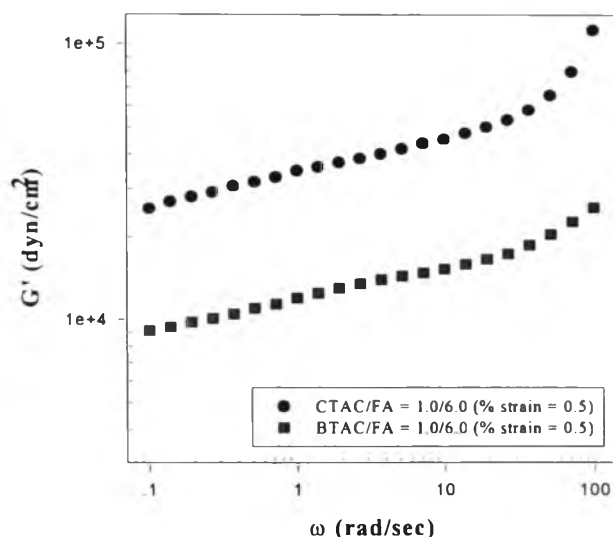


Figure 3. 22 Comparison of $G'(\omega)$ between CTAC/FA and BTAC/FA systems at high fatty alcohol concentration at equilibrium.

For high fatty alcohol concentration of 6.0% as shown in figure 3.22, $G'(\omega)$ of CTAC/FA system is higher than BTAC/FA system at all frequencies. This means that emulsion of the CTAC/FA system behaves more elastically than the BTAC/FA system. It is partly due to the network type formation of the CTAC/FA emulsion as shown in Figure 3.31c (compared to 3.31d).

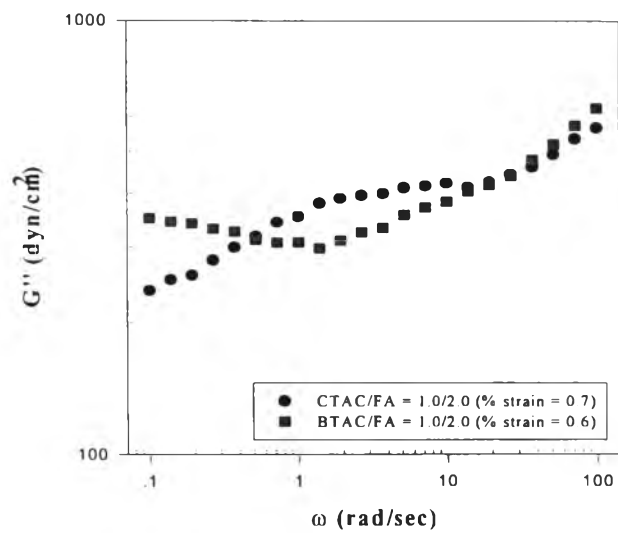


Figure 3.23 Comparison of $G''(\omega)$ between CTAC/FA and BTAC/FA systems at low fatty alcohol concentration at equilibrium.

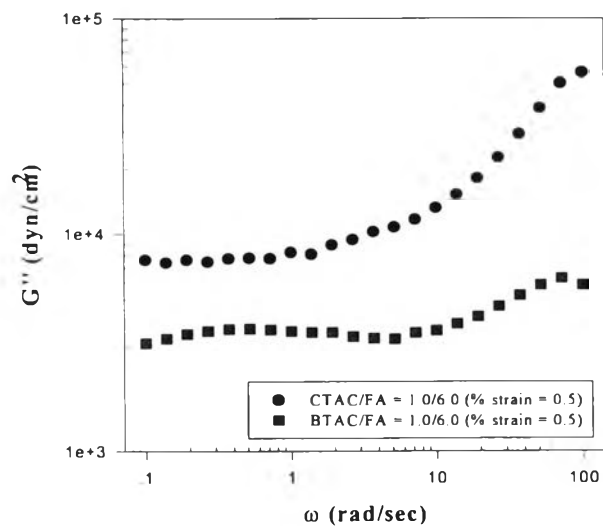


Figure 3.24 Comparison of $G''(\omega)$ between CTAC/FA and BTAC/FA systems at high fatty alcohol concentration at equilibrium.

In the case of $G''(\omega)$, we can observe that the $G''(\omega)$ of CTAC/FA system is higher than BTAC/FA system for low fatty alcohol concentration over all frequencies measured. For high fatty alcohol concentration, $G''(\omega)$ of CTAC/FA system is higher than BTAC/FA system at all frequencies. This occurs due to the same reason as $G'(\omega)$ of the CTAC/FA system as shown in Figure 3.24.

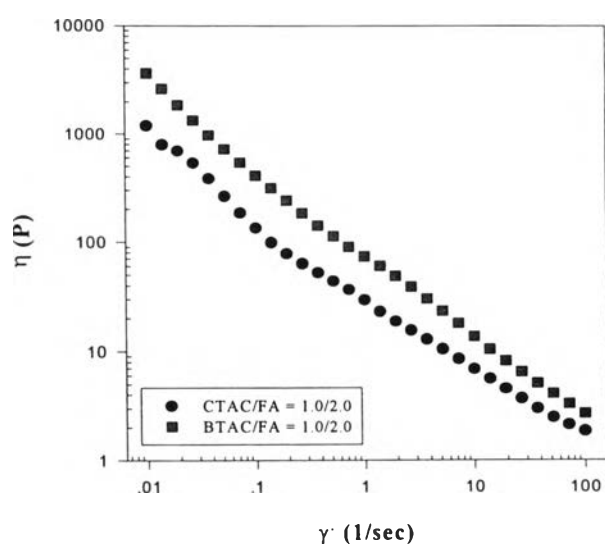


Figure 3.25 Comparison of η between CTAC/FA and BTAC/FA systems at low fatty alcohol concentration at equilibrium.

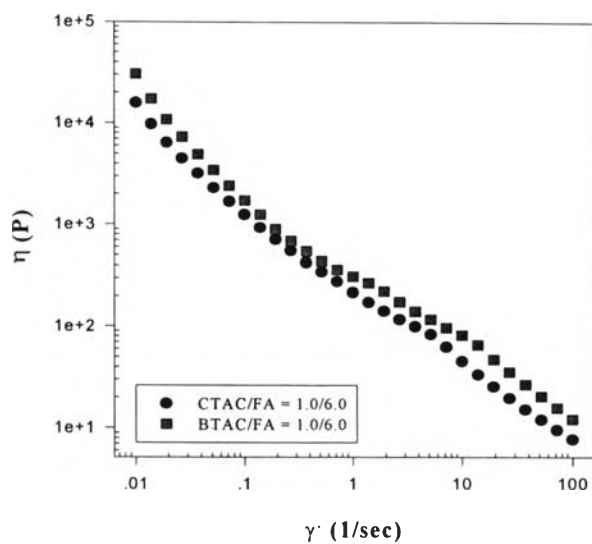


Figure 3.26 Comparison of η between CTAC/FA and BTAC/FA systems at high fatty alcohol concentration at equilibrium.

Figures 3.25 and 3.26 show the viscosity profiles of two emulsion systems. It can be seen that viscosity profile of BTAC/FA system is higher than CTAC/FA system at all frequency at both low and high fatty alcohol concentrations. This means that the longer chain length surfactant plays an important role by increasing the viscosity of the emulsion.

From previous section, emulsions were found to reach equilibrium about 2 weeks. We can define several important parameters: G_N^0 equal to $G'(\omega)$ at 100 rad/sec and it refers to the rigidity of material due to entanglement. η_0 is the viscosity at zero shear rate which is determined from η at a shear rate of 0.01 s^{-1} . τ_B is the Bingham stress which is the force that required to initiate the flow.

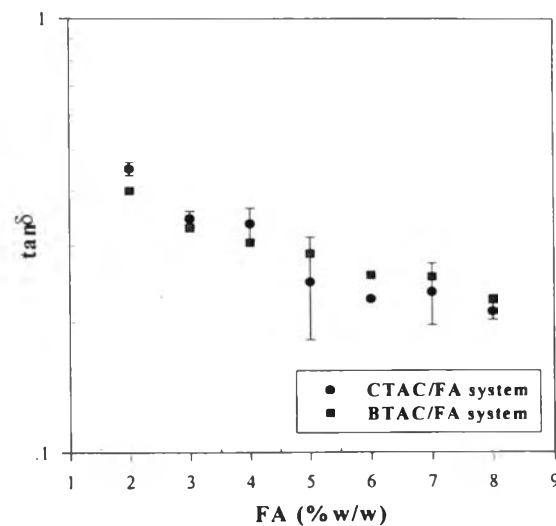


Figure 3.27 $\tan\delta$ vs. FA concentration of the CTAC/FA and BTAC/FA systems at equilibrium. ($\tan\delta$ at 100 rad/sec)

Figure 3.27 shows $\tan\delta$ versus FA concentration. $\tan\delta$ decreases with increasing FA content. It can be suggested that mixtures with larger FA content are relatively more elastic. $\tan\delta$ is also independent of the surfactant chain length.

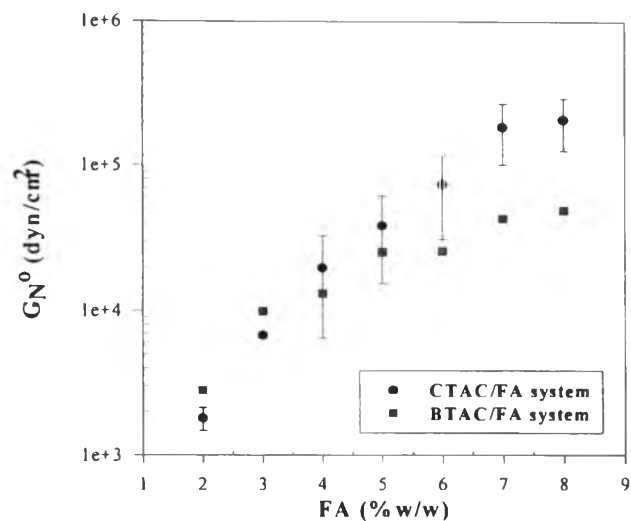


Figure 3.28 G_N^0 vs. FA concentration of the CTAC/FA and BTAC/FA systems at equilibrium. (G' at 100 rad/sec)

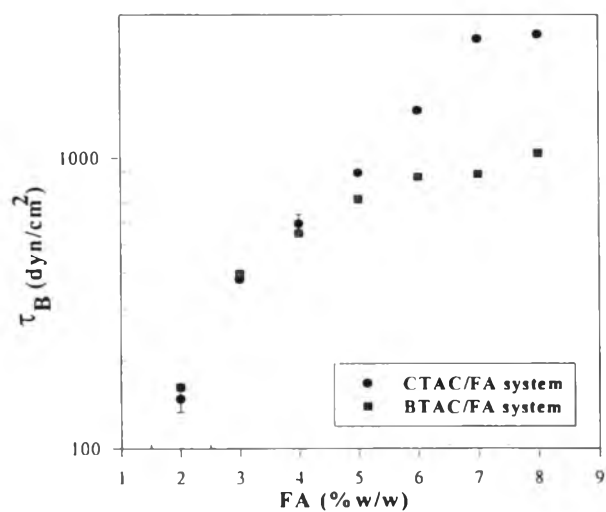


Figure 3.29 τ_B vs. FA concentration of the CTAC/FA and BTAC/FA systems at equilibrium.

Figures 3.28 and 3.29 show G_N^0 and τ_B versus FA concentration of the CTAC/FA system and the BTAC/FA system. The values of G_N^0 and τ_B of two emulsion systems are nearly the same in the range of FA 2.0-4.0% (low FA regime) and they increase with FA content until reaching the saturation value. The size of these two structures are comparable as shown in Figures 3.31 a,b. At high FA concentrations (5.0-8.0%), the values of G_N^0 and τ_B of the CTAC/FA system are higher than those of the BTAC/FA system. This is due to the fact that structure of CTAC/FA is the network type similar to the BTAC/FA system as shown in Figures 3.31 c,d.

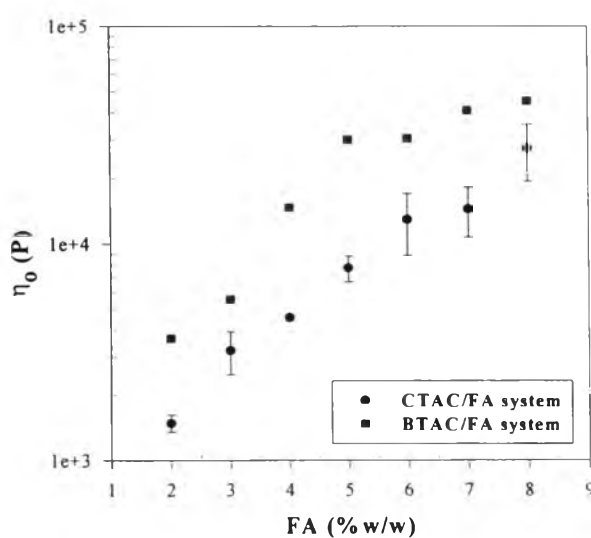


Figure 3.30 η_0 vs. FA concentration of the CTAC/FA and BTAC/FA systems at equilibrium.

Figure 3.30 shows the zero shear viscosity versus FA concentration of BTAC/FA and CTAC/FA systems. The zero shear viscosity of the BTAC/FA system is higher than the CTAC/FA system. It is partly due to long chain length of cationic surfactant. *Kevin (1994) reported that long-chain surfactant plays an important role in the increasing the viscosity of the products.*

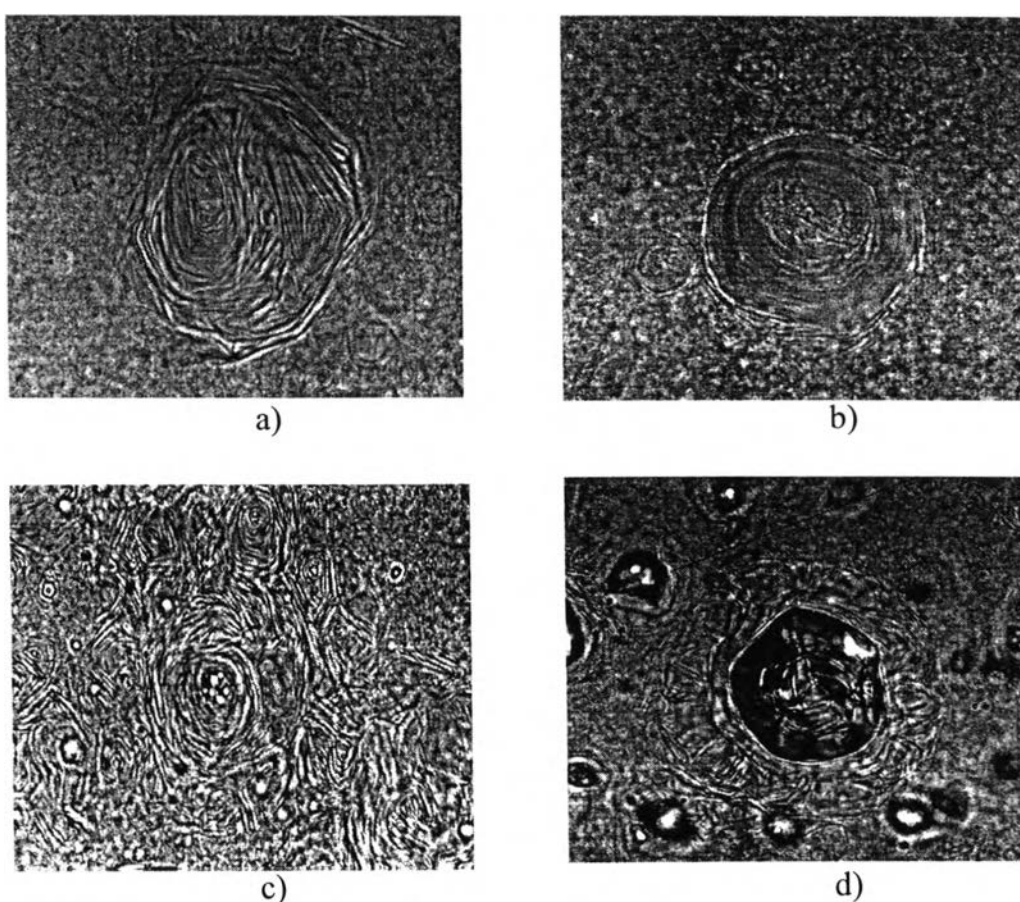


Figure 3.31 Comparison the structures of the CTAC/FA and BTAC/FA systems at low and high fatty alcohol concentrations at equilibrium: a) CTAC/FA = 1.0/2.0; b) BTAC/FA = 1.0/2.0; c) CTAC/FA = 1.0/6.0; d) BTAC/FA = 1.0/6.0.

3.4) Effect of Polymer Additive

We investigated the effect of polymer on the emulsion of CTAC/FA system by adding a fixed amount of the polymer HEC 0.5% and varied FA concentration.

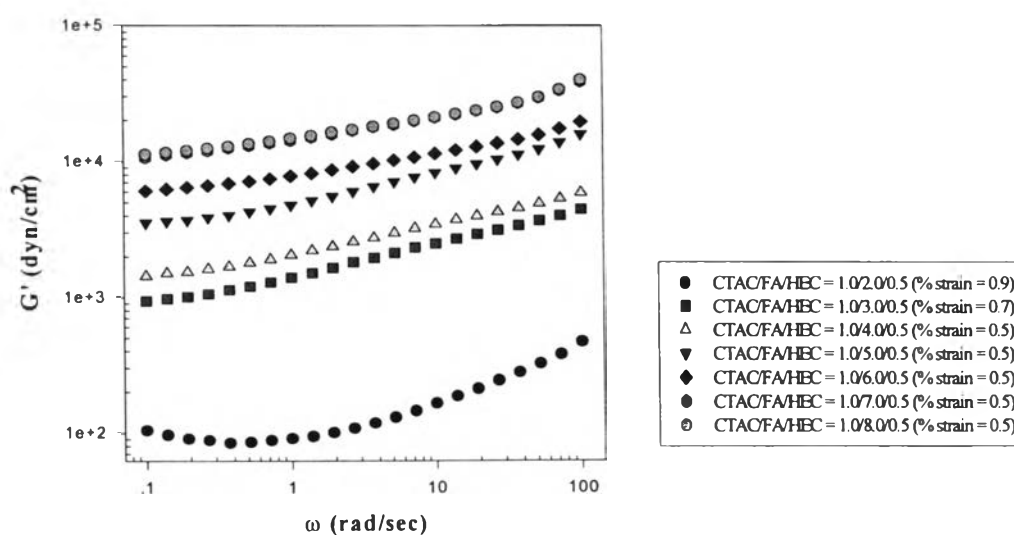


Figure 3.32 $G'(\omega)$ vs. frequency as a function of FA concentration for CTAC/FA/HEC system at equilibrium.

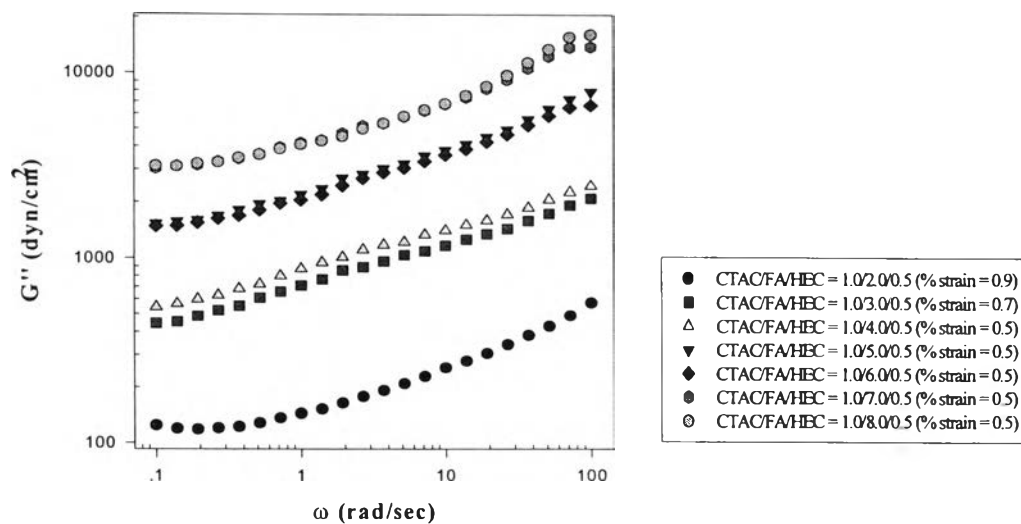


Figure 3.33 $G''(\omega)$ vs. frequency as a function of FA concentration for CTAC/FA/HEC system at equilibrium.

Figures 3.32 and 3.33 show $G'(\omega)$ and $G''(\omega)$ versus frequency as a function of FA concentration for CTAC/FA/HEC system. It can be seen that $G'(\omega)$ and $G''(\omega)$ increase with fatty alcohol concentration. This means that the elastic and loss moduli of emulsions increase with FA content.

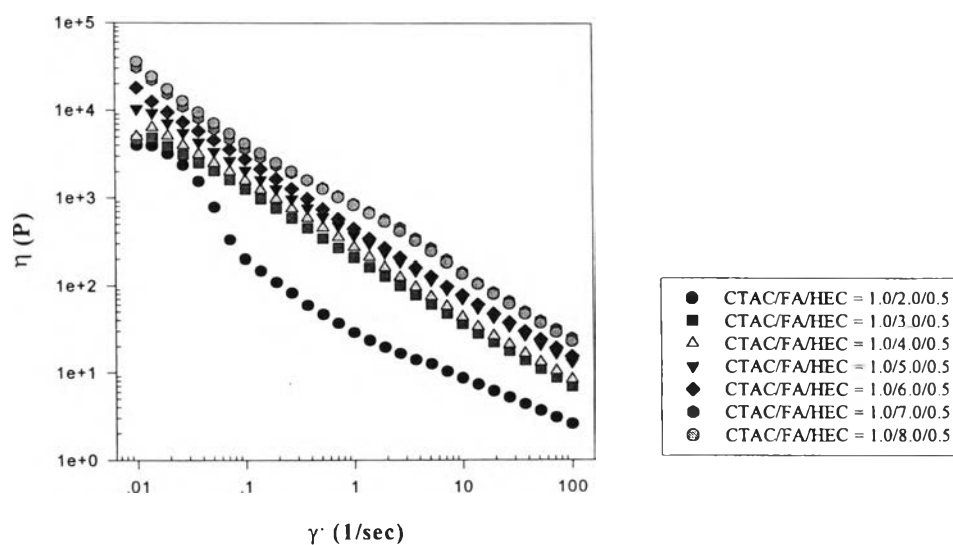


Figure 3.34 η vs. shear rate as a function of FA concentration for CTAC/FA/HEC system at equilibrium.

Figure 3.34 shows the viscosity profiles versus shear rate as a function of FA concentration for CTAC/FA/HEC systems. We found that the viscosity increases continuously with increasing FA concentration. We also found that the yield stress occurs for the CTAC/FA/HEC = 1.0/2.0/0.5. One possible is that at low FA content, the system is relatively inhomogeneous, containing discrete lamellar aggregates, but is more homogeneous at higher FA content (c.f. Fig. 3.11d versus 3.13d).

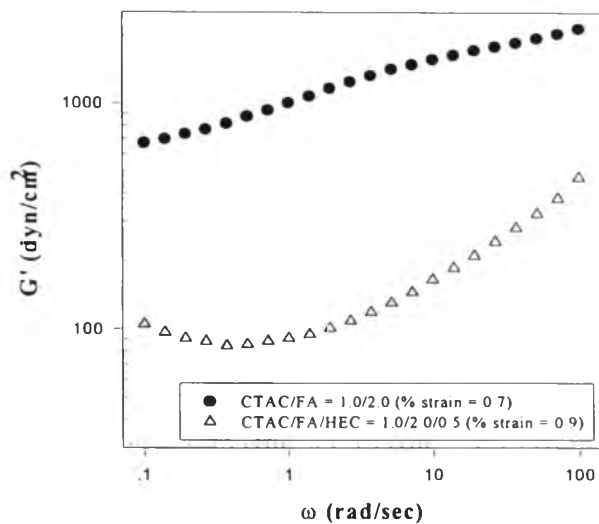


Figure 3.35 Comparison $G'(\omega)$ vs. frequency between the CTAC/FA and CTAC/FA/HEC systems at low fatty alcohol concentration at equilibrium.

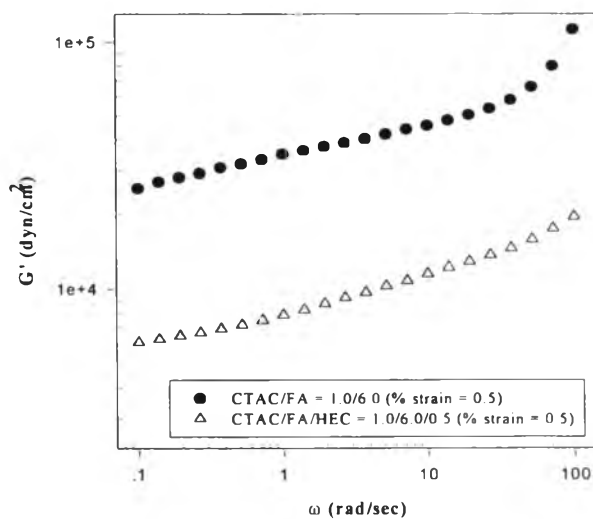


Figure 3.36 Comparison $G'(\omega)$ vs. frequency between the CTAC/FA and CTAC/FA/HEC systems at high fatty alcohol concentration at equilibrium.

Figures 3.35 and 3.36 show the comparison of the $G'(\omega)$ and the $G''(\omega)$ versus frequency between the CTAC/FA/HEC and CTAC/FA systems at low and high FA concentrations respectively. It can be clearly seen that both of $G'(\omega)$ and $G''(\omega)$ for the CTAC/FA system are above those of the CTAC/FA/HEC system over the entire range of frequency. The result suggests that the elasticity of CTAC/FA system tends to decrease due to addition of HEC polymer. Because the HEC polymer chains disrupt the aggregation of lamellar structure; therefore, its structures look like the partition of lamellar aggregate as shown in Figure 3.44 b,d.

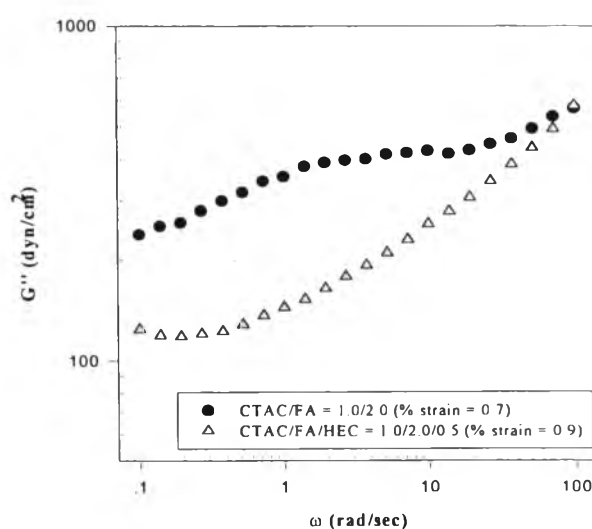


Figure 3.37 Comparison $G''(\omega)$ vs. frequency between the CTAC/FA and CTAC/FA/HEC systems at low fatty alcohol concentration at equilibrium.

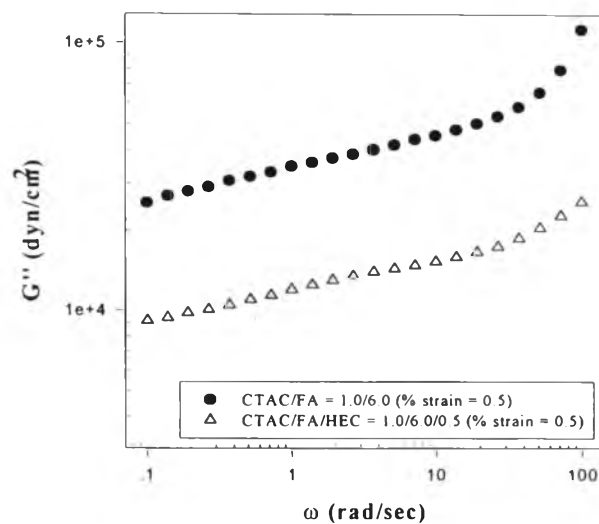


Figure 3.38 Comparison $G''(\omega)$ vs. frequency between the CTAC/FA and CTAC/FA/HEC systems at high fatty alcohol concentration at equilibrium.

Figure 3.37 and 3.38 show the comparison of the $G''(\omega)$ versus frequency between CTAC/FA/HEC and CTAC/FA systems at low and high FA concentrations respectively. We found that $G''(\omega)$ of both systems at low FA concentration show the same trend as $G'(\omega)$. But in the high frequency regime (relatively short time scale) at low FA concentration, $G''(\omega)$ of both systems are nearly the same.

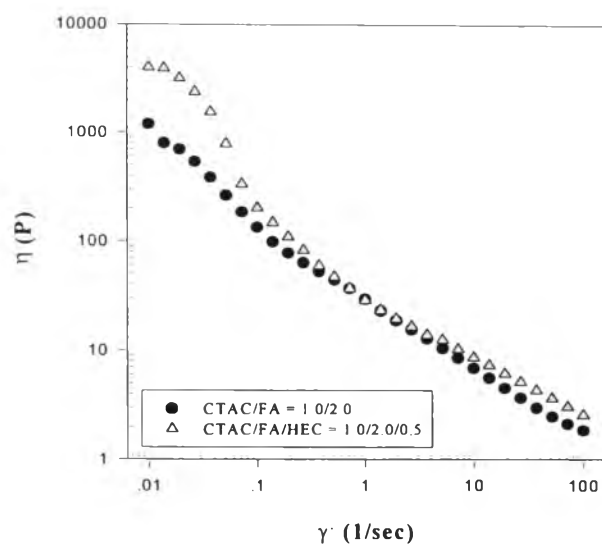


Figure 3.39 Comparison η vs. shear rate between the CTAC/FA and CTAC/FA/HEC systems at low fatty alcohol concentration at equilibrium.

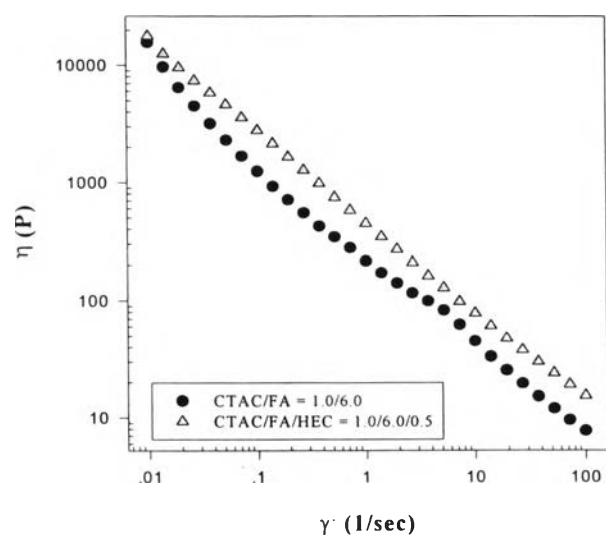


Figure 3.40 Comparison η vs. shear rate between the CTAC/FA and CTAC/FA/HEC systems at high fatty alcohol concentration at equilibrium.

Figure 3.39 and 3.40 show the viscosity profiles for CTAC/FA/HEC and CTAC/FA systems at low and high FA concentration. It can be seen that the viscosity of the CTAC/FA/HEC system at high and low FA concentration falls above the CTAC/FA system over the entire range of shear rate. We can notice that the yield stress occurs at low shear rate for the CTAC/FA/HEC = 1.0/2.0/0.5 system. This result can be supported by the micrographs as shown in Figure 3.11d that yield stress occur probably due to the formation network structure.

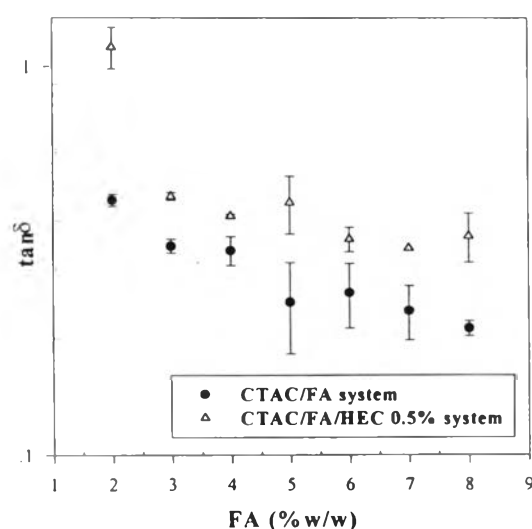


Figure 3.41 $\tan\delta$ vs. FA concentration of the CTAC/FA and CTAC/FA/HEC systems at equilibrium. ($\tan\delta$ at 100 rad/sec)

Figure 3.41 shows the $\tan\delta$ versus FA concentration of two emulsion systems. One is CTAC/FA system without polymer, another one is the system with polymer 0.5%. $\tan\delta$ decrease with FA concentration. This means that the emulsion elasticity increases with FA concentration. $\tan\delta$ of the CTAC/FA

system with the HEC polymer additive is higher than the system without polymer at any FA concentration. It means that the polymer will play a major role to disrupt the aggregation of lamellar structure making the emulsions more liquidlike.

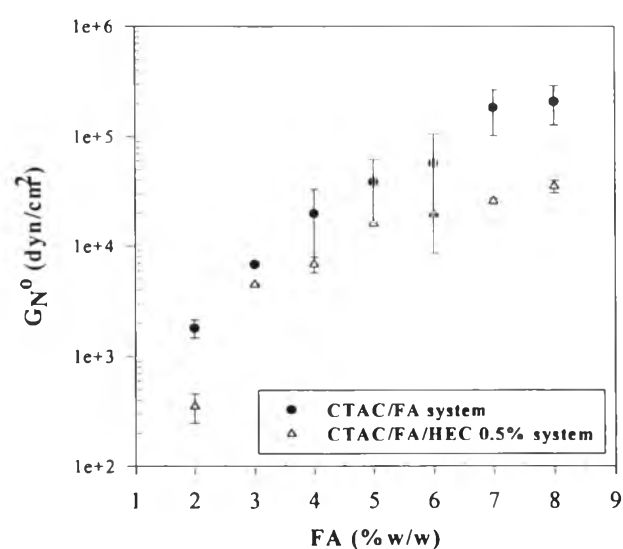


Figure 3.42 G_N^0 vs. FA concentration of the CTAC/FA and CTAC/FA/HEC systems at equilibrium. (G' at 100 rad/sec)

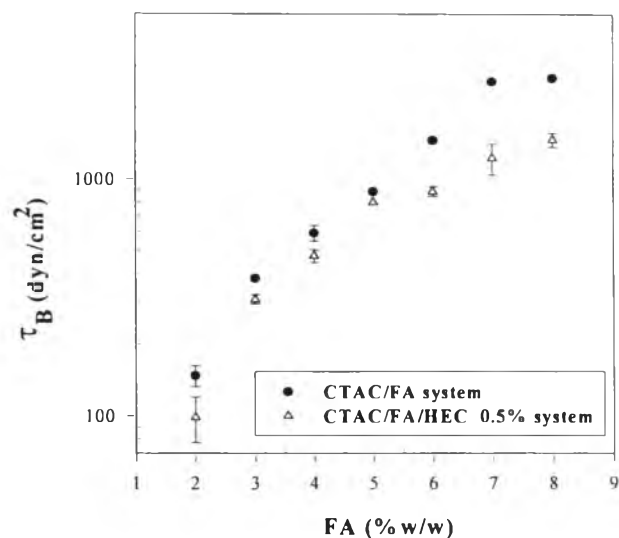


Figure 3.43 τ_B vs. FA concentration of the CTAC/FA and CTAC/FA/HEC systems at equilibrium.

Figure 3.42 and 3.43 show G_N^0 and τ_B versus FA concentration of the system CTAC/FA and CTAC/FA/HEC 0.5%. The values of G_N^0 and τ_B increase with FA content until reaching the saturation value. At high FA concentration, G_N^0 of both systems are nearly the same because the structure sizes are comparable. At high FA concentration, G_N^0 and τ_B of the CTAC/FA system increase away from those of the BTAC/FA system because the structure of CTAC/FA system without polymer has both large structure size and the formation of network type as shown in Figure 3.44.

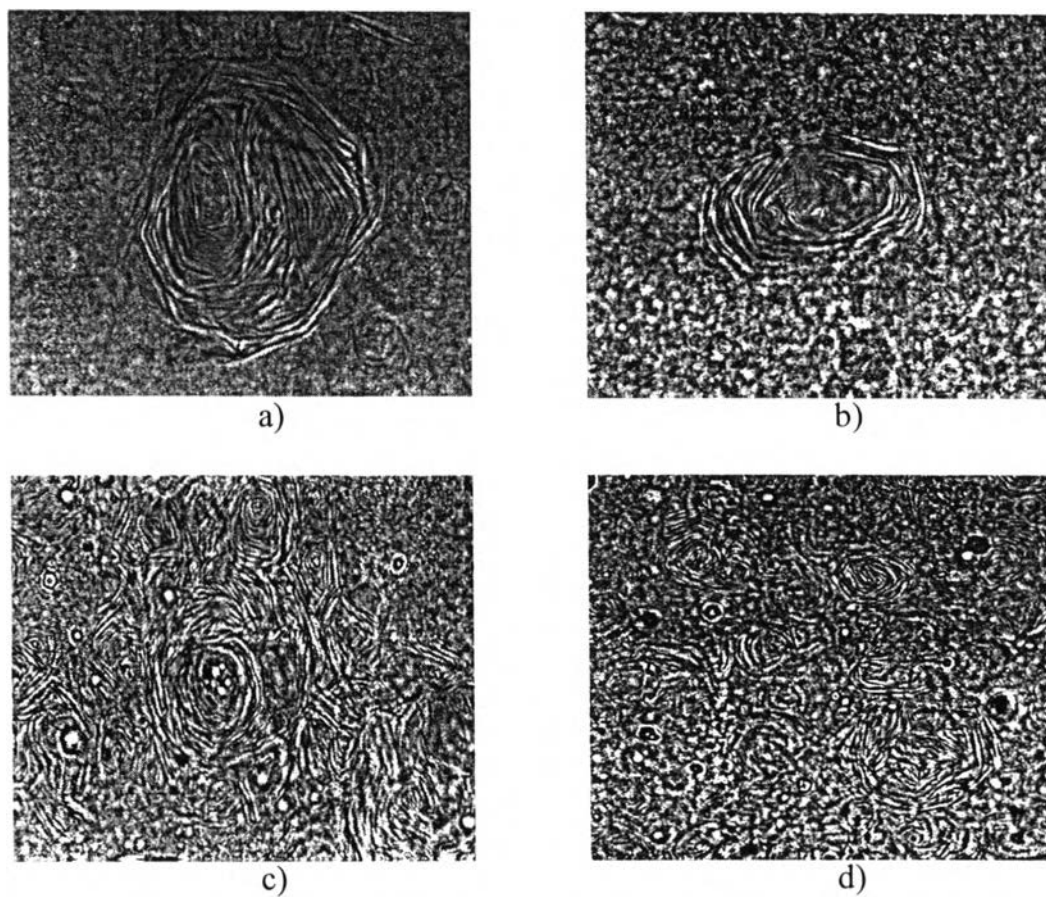


Figure 3.44 Comparison the structures of the CTAC/FA and CTAC/FA/HEC systems at low and high fatty alcohol concentrations at equilibrium: a) CTAC/FA = 1.0/2.0; b) CTAC/FA/HEC = 1.0/2.0/0.5; c) CTAC/FA = 1.0/6.0; d) CTAC/FA/HEC = 1.0/6.0/0.5.

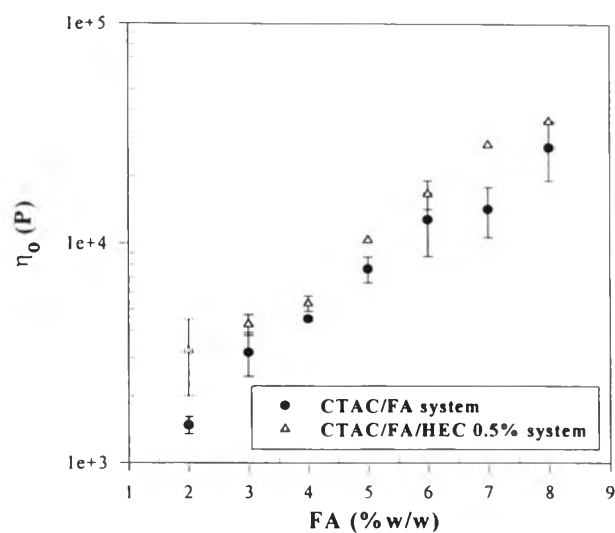


Figure 3.45 η_0 vs. FA concentration of the CTAC/FA and CTAC/FA/HEC systems at equilibrium.

Figure 3.45 shows the zero shear viscosity versus FA concentration of the CTAC/FA/HEC and the CTAC/FA systems. The zero shear rate viscosity of CTAC/FA with polymer is higher than the system without polymer at any fatty alcohol concentration. It can be said that the polymer increases the emulsion viscosity.

3.5) Effect of Annealing

In this experiment, the emulsion systems were annealed at 40, 53, and 80 °C respectively at the stirring speed 110 rpm for 15 minutes. After annealing, the emulsions were cooled down naturally toward room temperature and we studied the rheological and optical properties as a function of aging time. The zero shear viscosity was used to detect the changes in emulsion properties.

3.5.1 Emulsion of CTAC/FA systems

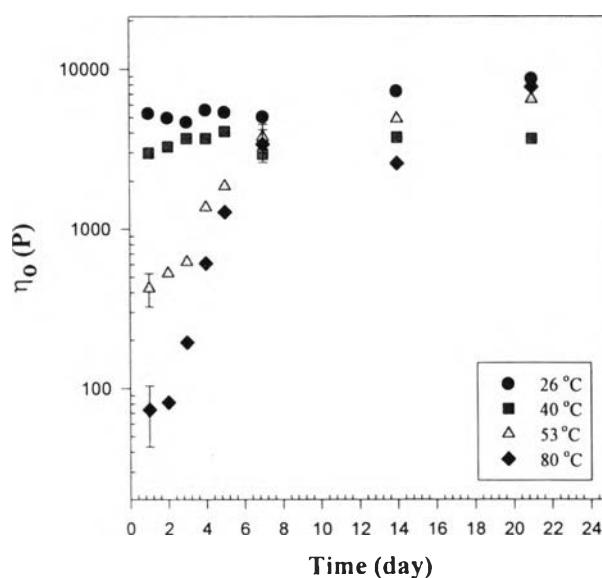


Figure 3.46 Zero shear rate viscosity vs. aging time with various annealing temperatures for the CTAC/FA = 1.0/2.0 system.

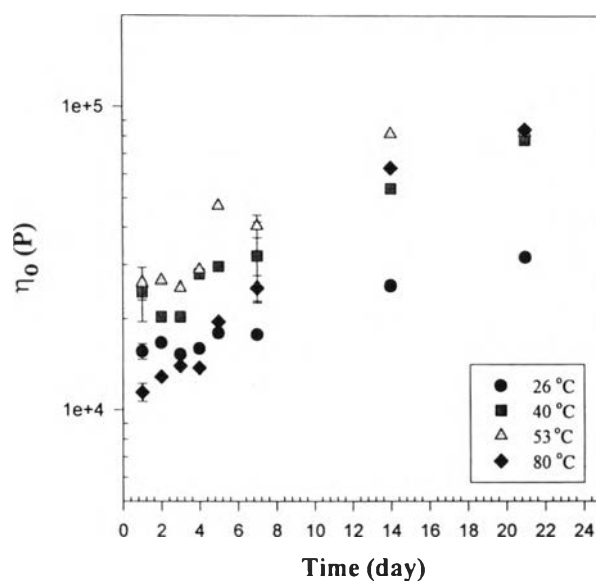


Figure 3.47 Zero shear rate viscosity vs. aging time with various annealing temperatures for the CTAC/FA = 1.0/4.0 system.

Figure 3.46 shows the zero shear viscosity versus aging time at various annealing temperatures for the CTAC/FA = 1.0/2.0 system. It can be seen that after annealing at 40 °C, the zero shear viscosity slightly increases until reaching equilibrium condition. This result corresponds to the micrographs shown in Figure 3.48. The structure size does not change relative to the original size. After annealing at 53 °C, the zero shear viscosity drops down by a factor of 10 from the initial value before annealing at the first day. After that it returns to the initial value until reaching equilibrium. Figure 3.49 shows the corresponding micrograph structures for CTAC/FA = 1.0/2.0 annealed at 53 °C. After annealing at 53 °C, the structure size decreases at the first day because this temperature is high enough to melt some part of lamellar structure which can be attributed to

the reduction of structure size. Later on, the structure size returns to the original size about 21 days. The above trend is also observed, after annealing at 80 °C, the zero shear viscosity drops sharply by 60 times at first day and returns to the initial value within about 21 days. The micrographs also show the same trend that there is a decrease in structure size after annealing at 80 °C and then it returns to the initial size until reaching equilibrium condition as shown in Figure 3.50.

In the case of emulsion system for CTAC/FA (1.0/4.0) at high FA concentration, after annealing at 40 and 53 °C, the zero shear viscosities are higher than the emulsion without annealing. They increase with aging time until reaching equilibrium within 21 days. The micrographs are clearly seen in Figures 3.51 and 3.52. After annealing at 40 and 53 °C, some FA droplets were found. The viscosities of emulsions after annealing at 40 and 53 °C are higher than those of emulsions without annealing. This is probably due to droplet of FA. Annealing at 80 °C, the zero shear viscosity slightly drops down from the initial value and increases the unannealed emulsion and reaches equilibrium at 21 days. Figure 3.53 shows the corresponding micrographs of CTAC/FA = 1.0/4.0 after annealing at 80 °C. Clearly, it can be seen that the structure changes from lamellar aggregate to the small droplets of FA surrounded with lamellar structure.

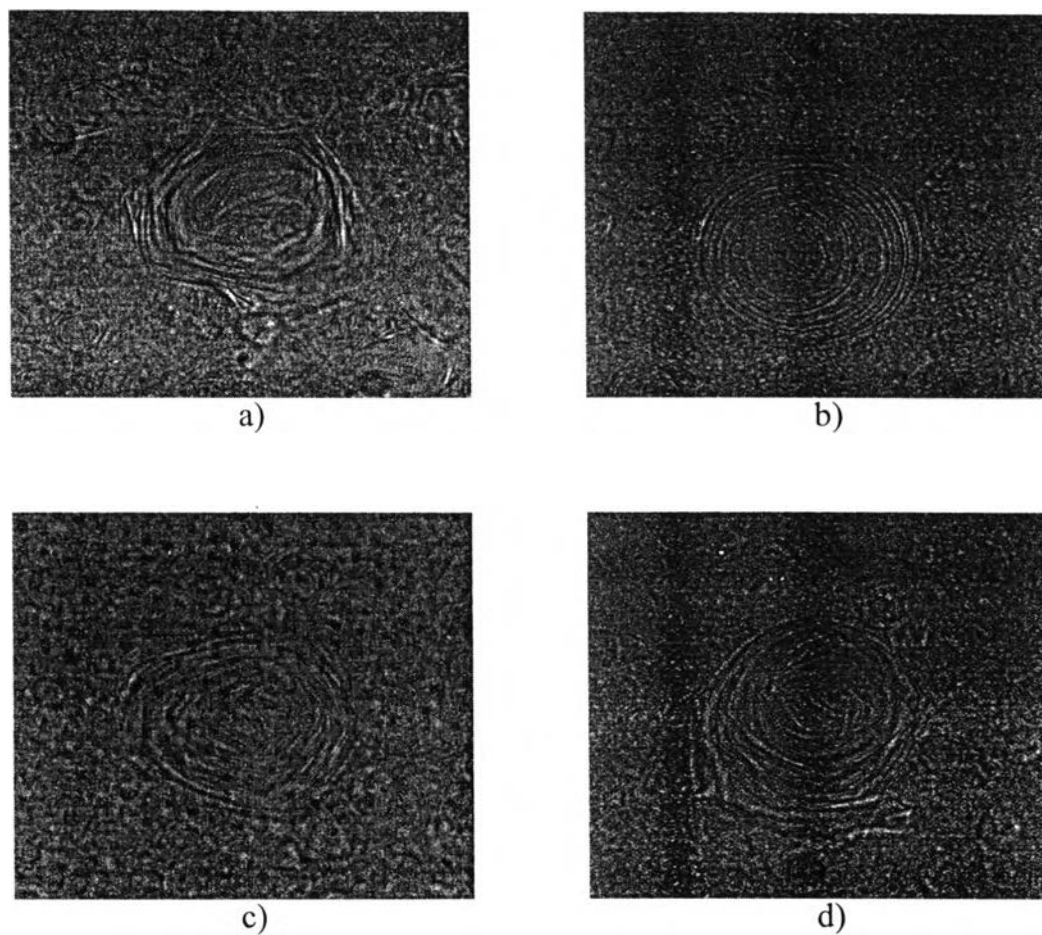


Figure 3.48 Micrographs of the CTAC/FA = 1.0/2.0 with annealing at 40 °C :
a) without annealing; b) after aging 1 day; c) after aging 7 days; d) after aging 14 days.

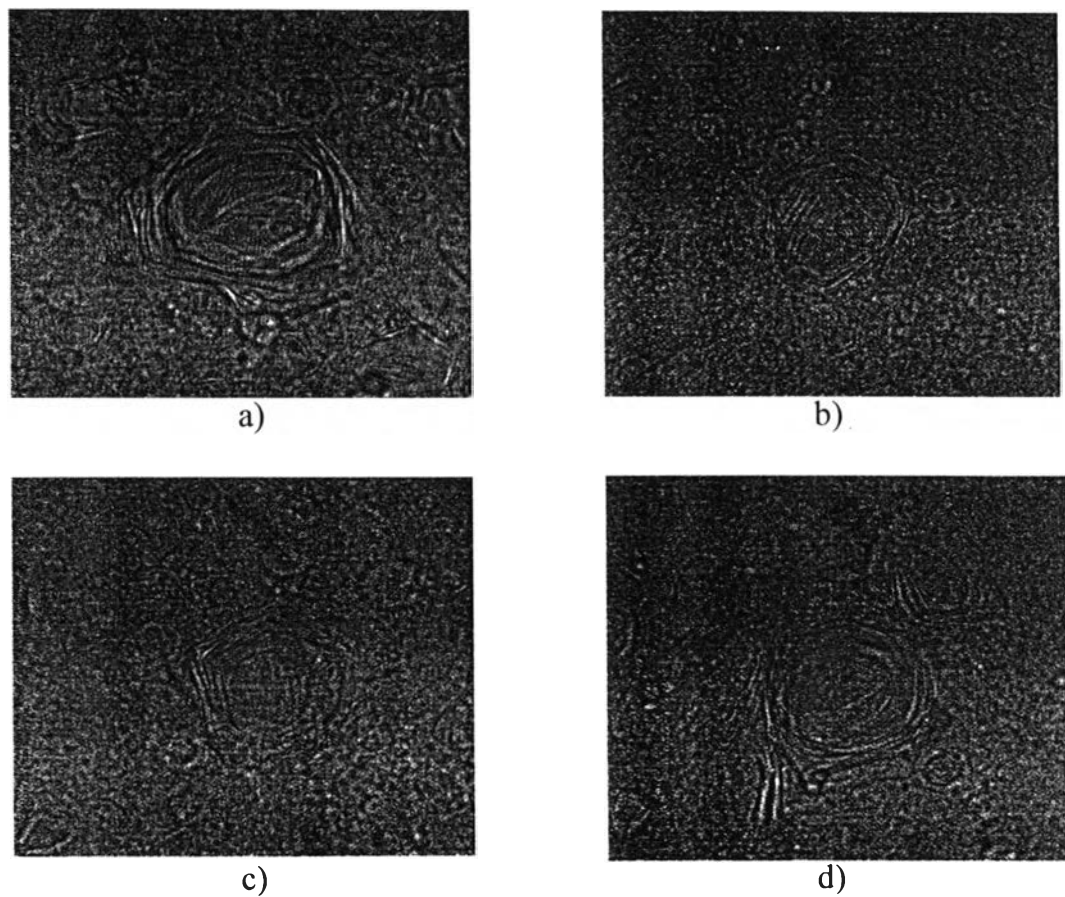


Figure 3.49 Micrographs of the CTAC/FA = 1.0/2.0 with annealing at 53 °C :
a) without annealing; b) after aging 1 day; c) after aging 7 days; d) after aging 14 days.

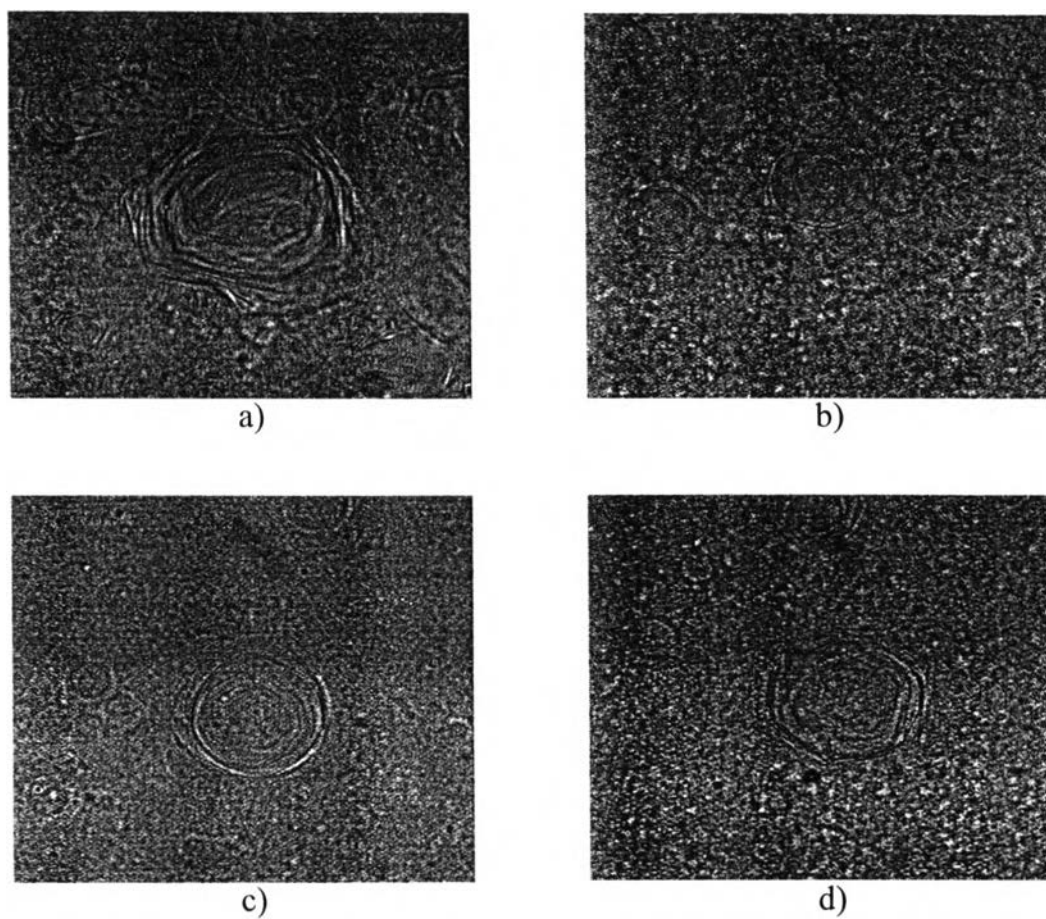


Figure 3.50 Micrographs of the CTAC/FA = 1.0/2.0 with annealing at 80 °C :
a) without annealing; b) after aging 1 day; c) after aging 7 days; d) after aging 14 days.

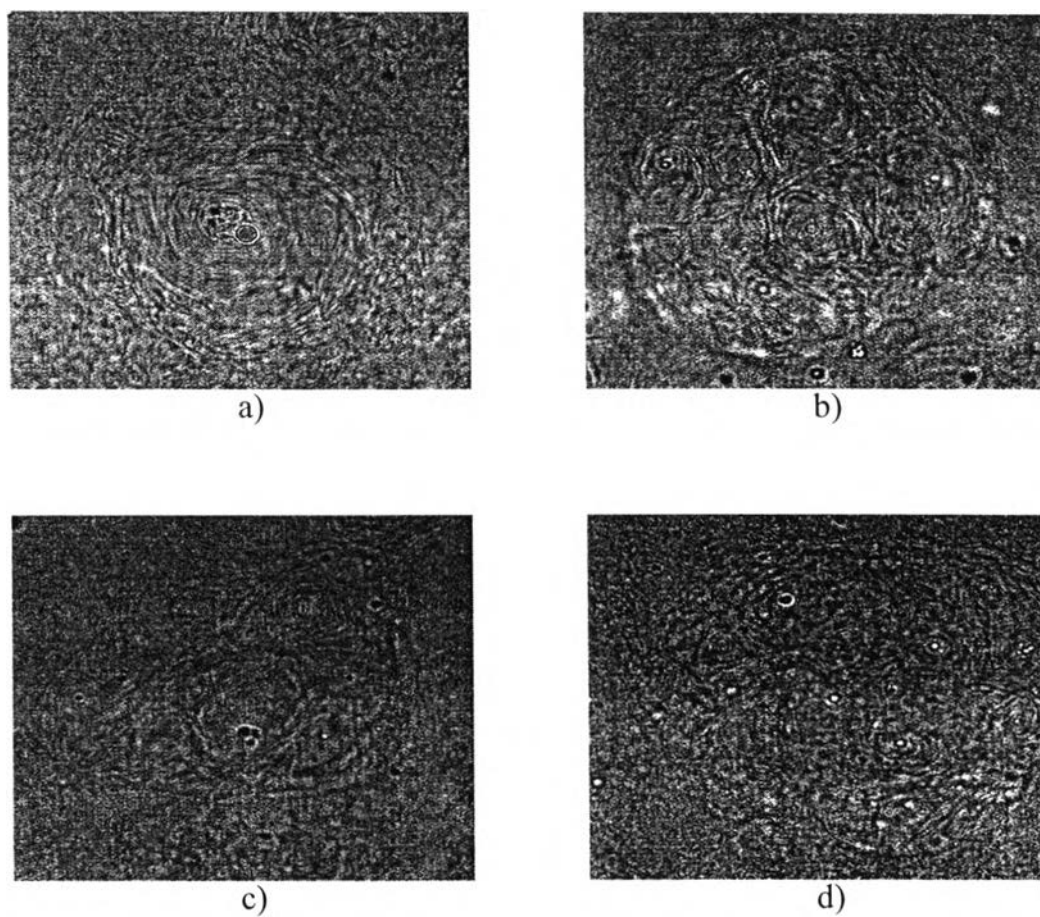


Figure 3.51 Micrographs of the CTAC/FA = 1.0/4.0 with annealing at 40 °C :
a) without annealing; b) after aging 1 day; c) after aging 7 days; d) after aging 14 days.

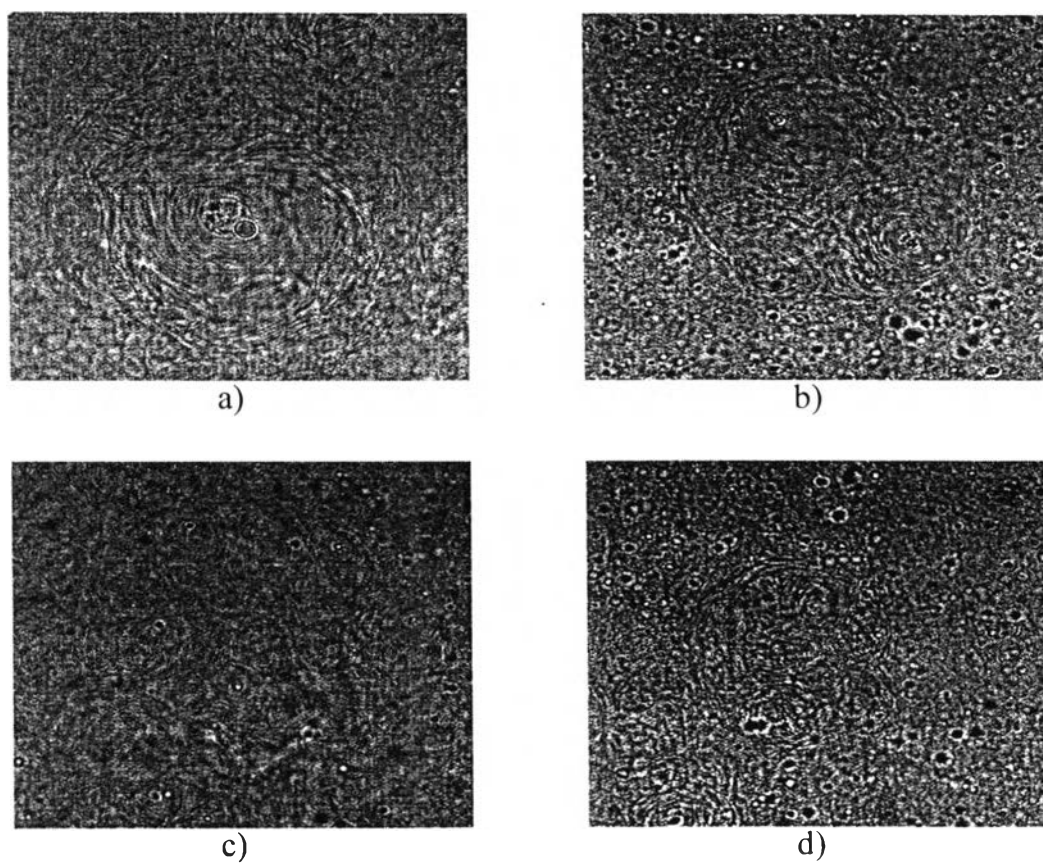


Figure 3.52 Micrographs of the CTAC/FA = 1.0/4.0 with annealing at 53 °C :
a) without annealing; b) after aging 1 day; c) after aging 7 days; d) after aging 14 days.

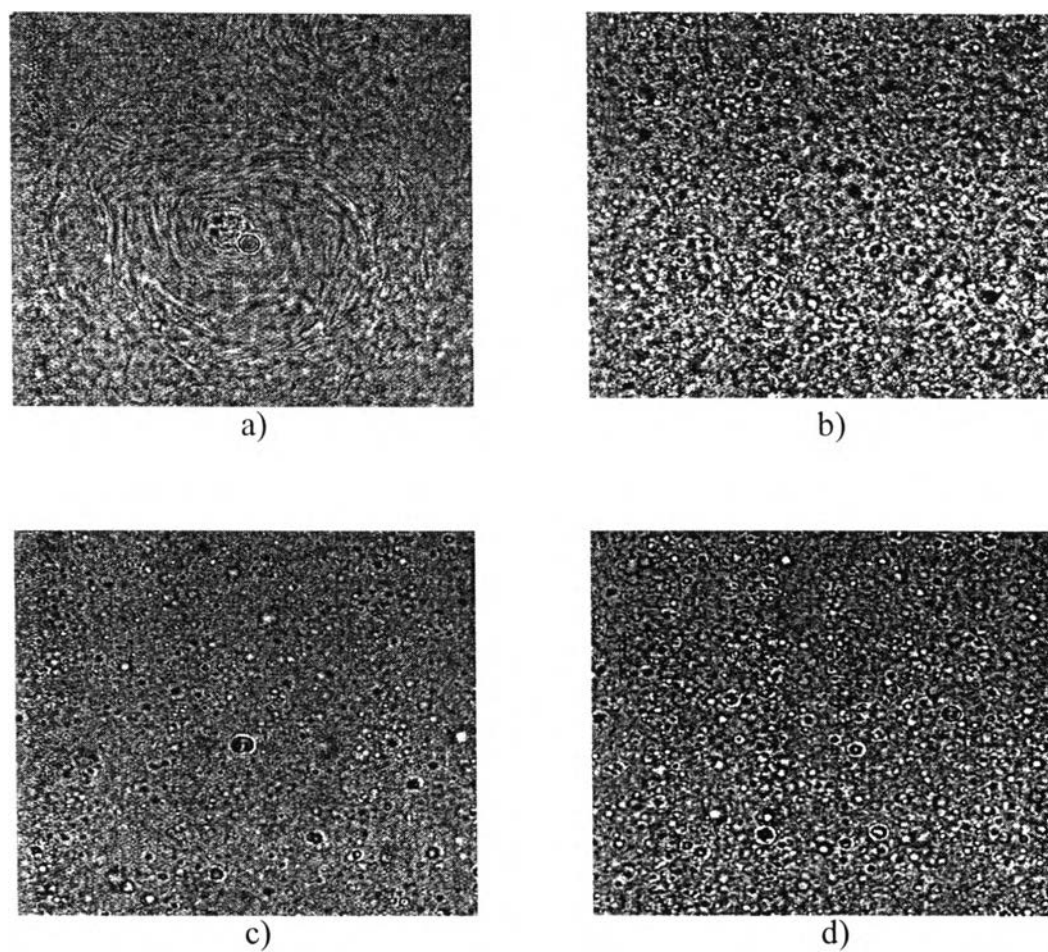


Figure 3.53 Micrographs of the CTAC/FA = 1.0/4.0 with annealing at 80 °C :
a) without annealing; b) after aging 1 day; c) after aging 7 days; d) after aging 14 days.

3.5.2 Emulsion of BTAC/FA systems

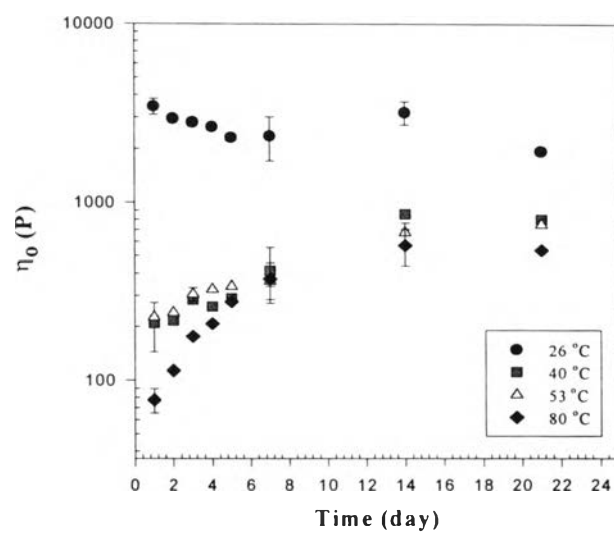


Figure 3.54 Zero shear rate viscosity vs. aging time with various annealing temperature for the BTAC/FA = 1.0/2.0 system.

Similar results were obtained for the emulsion of the BTAC/FA system. We can observe that after annealing at 40, and 53 °C, the zero shear viscosities drop down by a factor of 15 at the first day and return to the initial value until reaching equilibrium condition. After annealing at 80 °C, the viscosity shows the same trend as those of the CTAC/FA system.

Figure 3.56-3.58 shows the micrographs of the BTAC/FA = 1.0/2.0 emulsion annealed at 40, 53, and 80 °C respectively. The higher the annealing temperature, the more drops of FA can be observed.

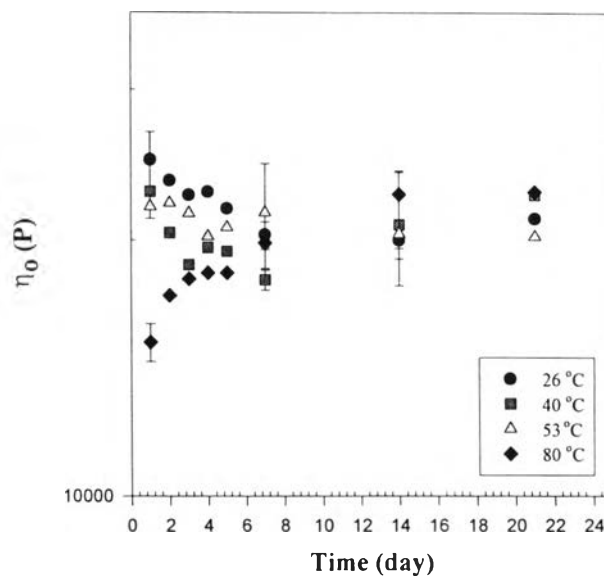


Figure 3.55 Zero shear rate viscosity vs. aging time with various annealing temperature for the BTAC/FA = 1.0/4.0 system.

Figure 3.55 shows zero shear rate viscosity versus aging time at various annealing temperatures for the BTAC/FA =1.0/4.0 system. After annealing at 40 and 53 °C, the zero shear viscosities decrease in period of 7 days then reach equilibrium within 21 days. These results correspond to the micrographs as shown in Figure 3.59 and 3.60. It can be seen that its structure size decrease after annealing at 40 and 53 °C until the structure size remains the same at the equilibrium condition. In the case of annealing at 80 °C, the zero shear viscosity drops dramatically and returns to the initial value until reaching equilibrium. The micrograph as shown in Figure 3.61 can support this result. After annealing at 80 °C, the structure change from large droplets of FA surrounded with lamellar aggregates to small FA droplets surrounded with lamellar aggregates. Later on the amount of FA droplets reduces when the emulsion was aged.

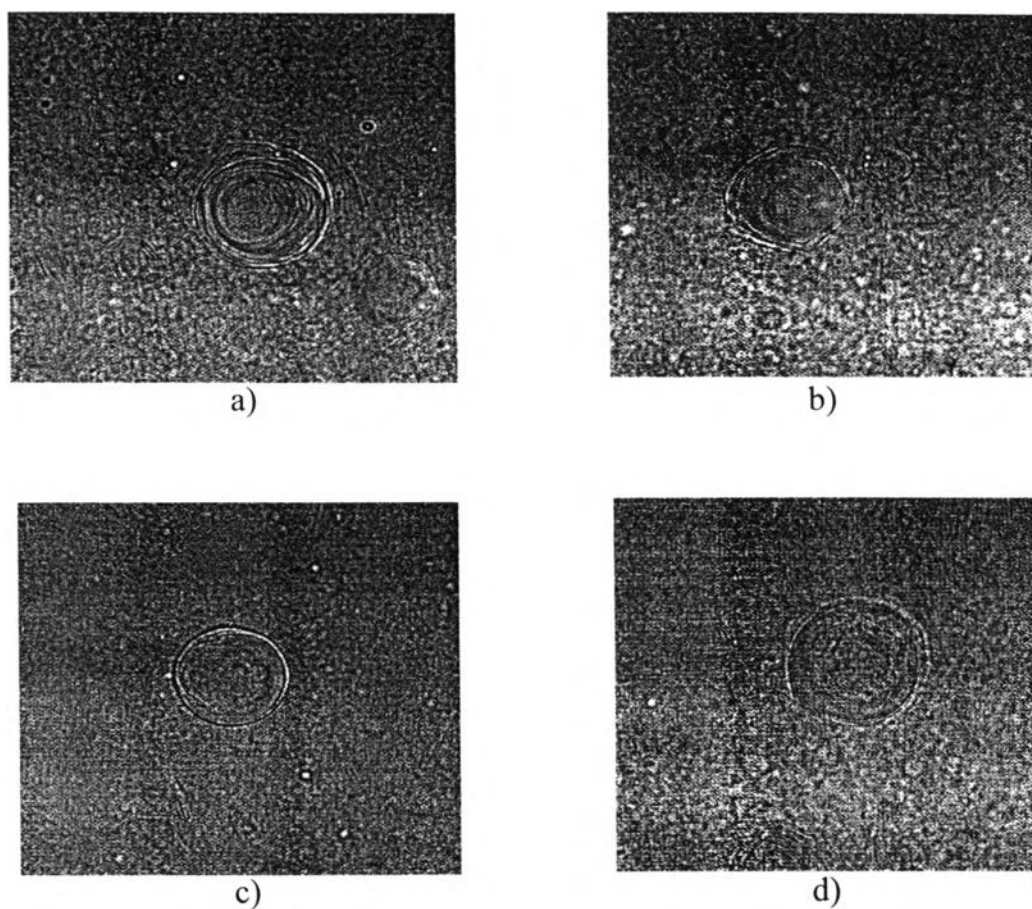


Figure 3.56 Micrographs of the BTAC/FA = 1.0/2.0 with annealing at 40 °C :
a) without annealing; b) after aging 1 day; c) after aging 7 days; d) after aging 14 days.

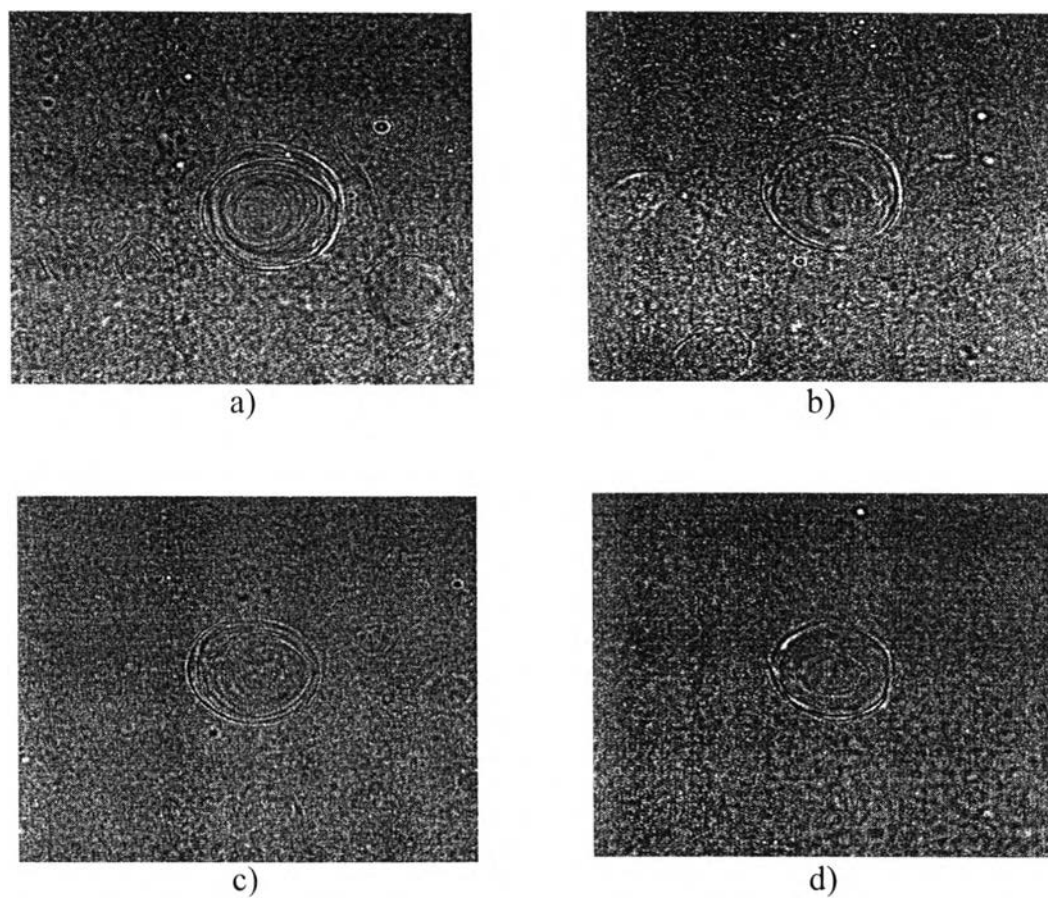


Figure 3.57 Micrographs of the BTAC/FA = 1.0/2.0 with annealing at 53 °C :
a) without annealing; b) after aging 1 day; c) after aging 7 days; d) after aging 14 days.

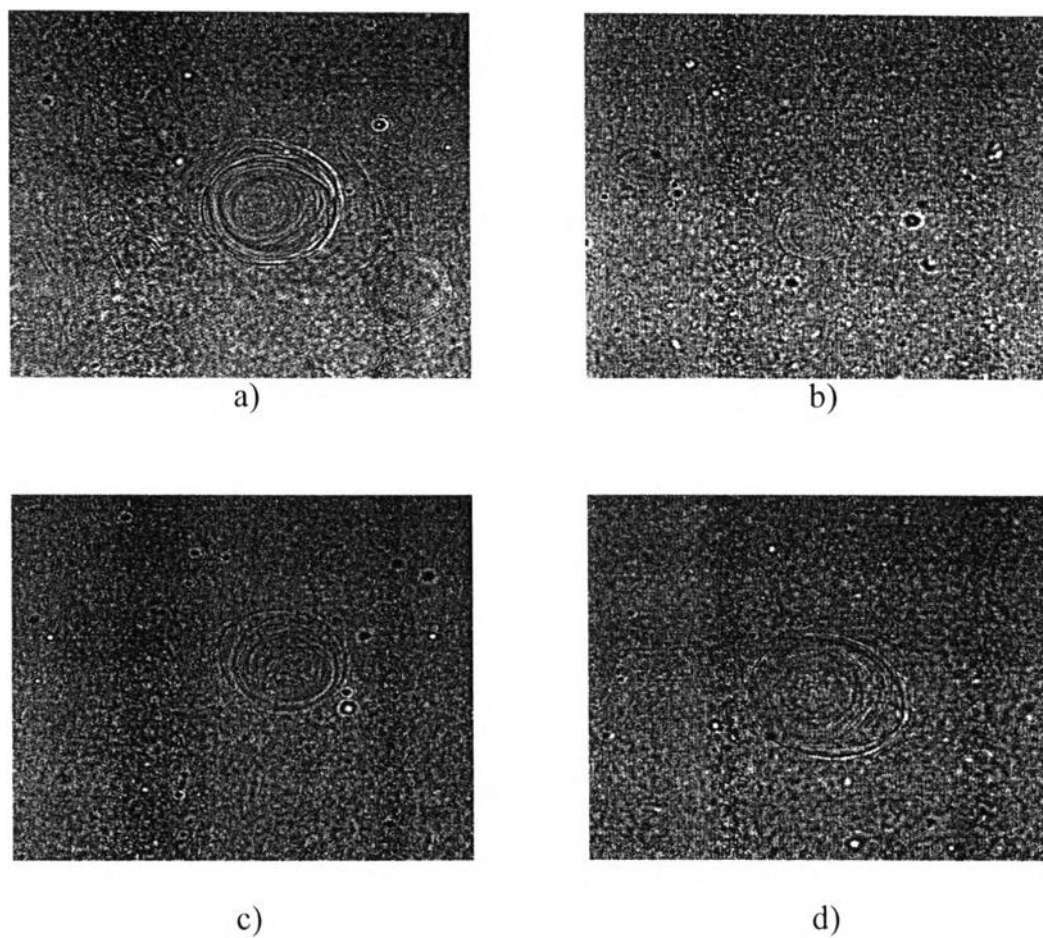


Figure 3.58 Micrographs of the BTAC/FA = 1.0/2.0 with annealing at 80 °C :
a) without annealing; b) after aging 1 day; c) after aging 7 days; d) after aging 14 days.

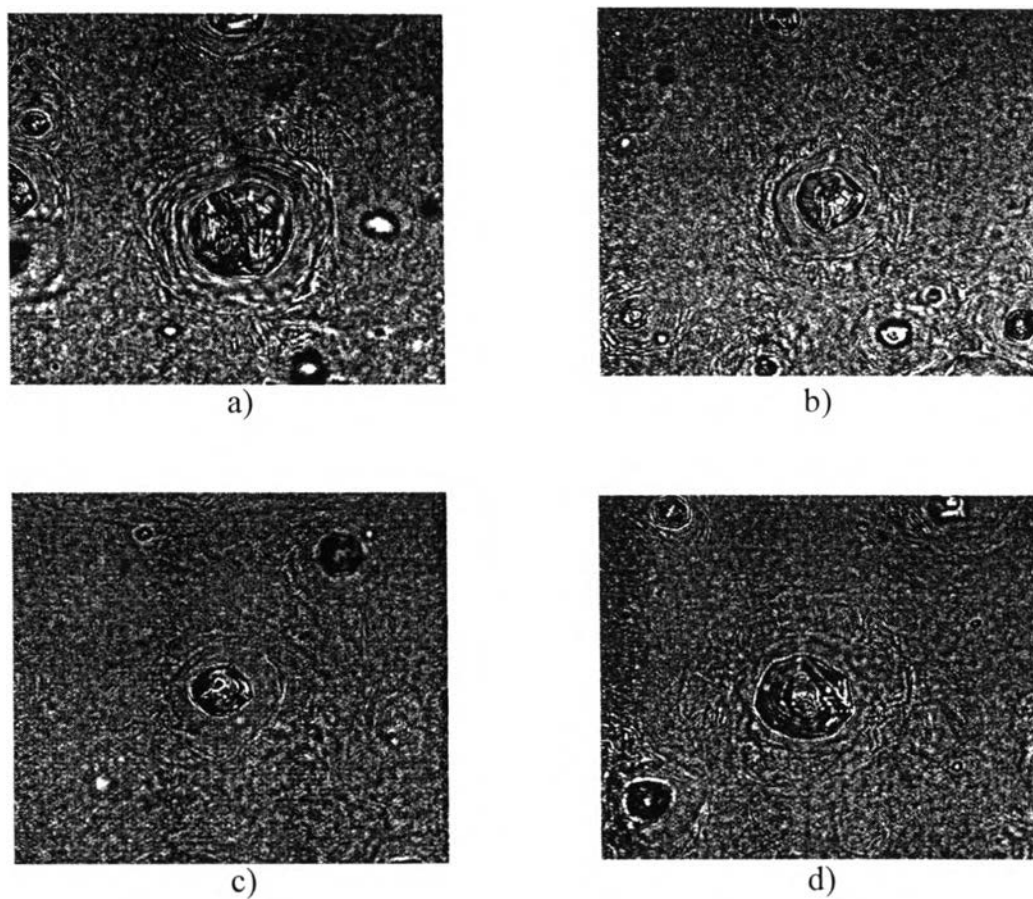


Figure 3.59 Micrographs of the BTAC/FA = 1.0/4.0 with annealing at 40 °C :
a) without annealing; b) after aging 1 day; c) after aging 7 days; d) after aging 14 days.

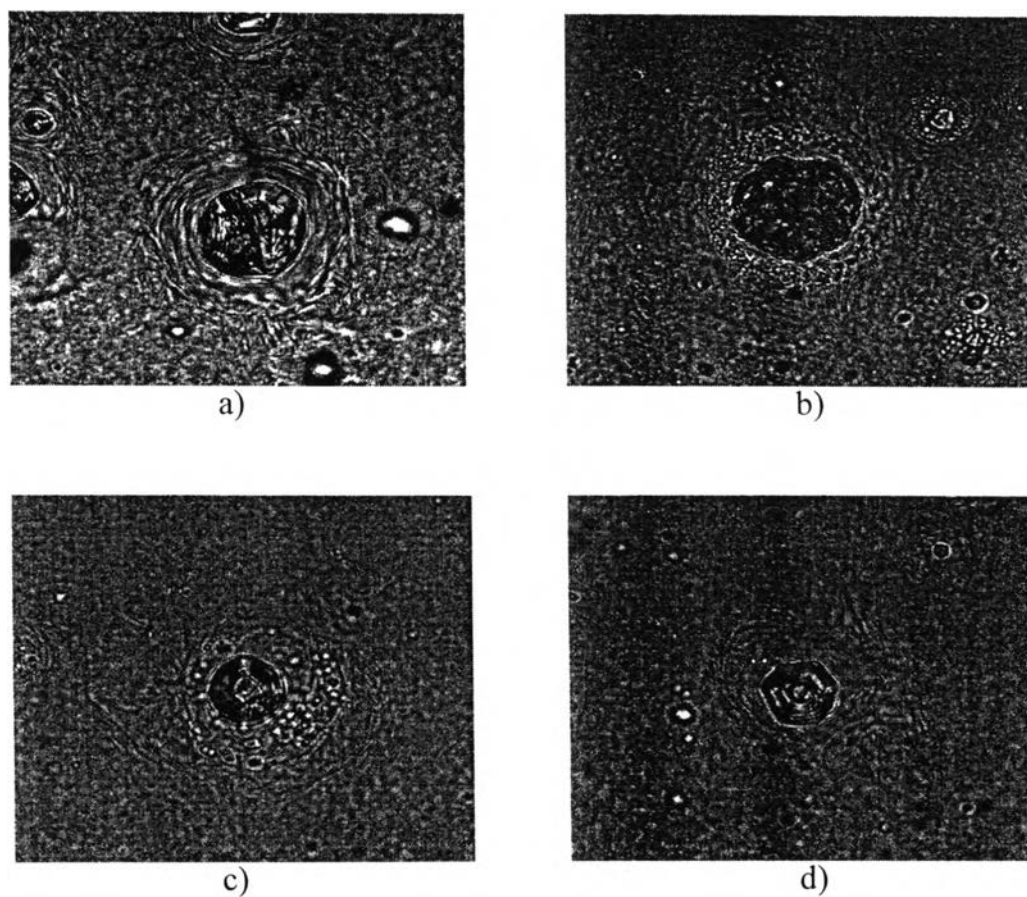


Figure 3.60 Micrographs of the BTAC/FA = 1.0/4.0 with annealing at 53 °C :
a) without annealing; b) after aging 1 day; c) after aging 7 days; d) after aging 14 days.

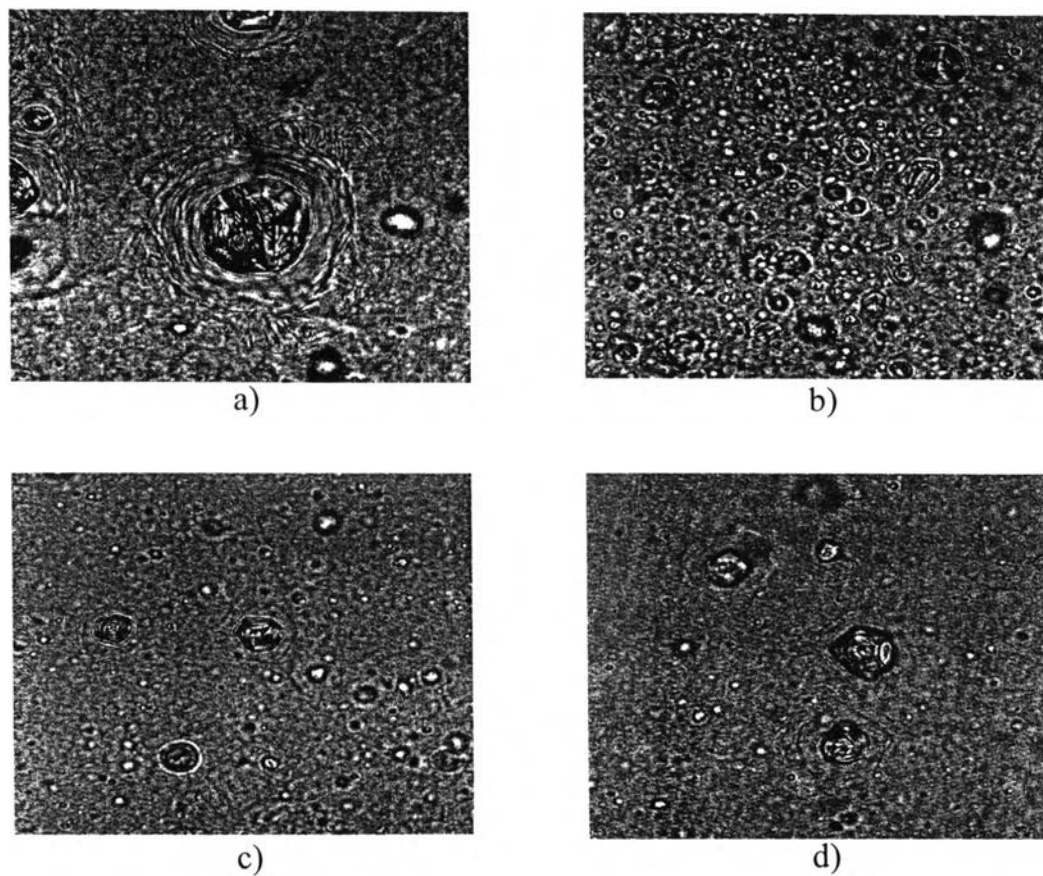


Figure 3.61 Micrographs of the BTAC/FA = 1.0/4.0 with annealing at 80 °C :
a) without annealing; b) after aging 1 day; c) after aging 7 days; d) after aging 14 days.